SciMedCentral

JSM Clinical Pharmaceutics

Research Article

Reduction of Nano-berberin affinity to human serum albumin in the presence of holo-transferrin: Spectroscopic, zeta potential and molecular modeling investigations

Atena Sharifi-Rad[1], Jamshid Mehrzad[1]*, Majid Darroudi[2], Mohammad Reza Saberi[3], Jamshidkhan Chamani[4]*

[1]*Department of Biochemistry, Faculty of Sciences, Neyshabur Branch, Islamic Azad University, Neyshabur, Iran*

[2] *Nuclear Medicine Research Center, Mashhad University of Medical Sciences, Mashhad, Iran*

[3]*Department of Medical Chemistry, School of Pharmacy, Mashhad University of Medical Sciences, Mashhad, Iran*

[4]*Department of Biology, Faculty of Sciences, Mashhad Branch, Islamic Azad University, Mashhad, Iran*

***Corresponding author**

JamshidMehrzad, JamshidkhanChamani. Tel:+98511 8437107 Fax: +98511 8424020 E-mail: mehrzadjam@yahoo.com; chamani.j@ut.ac.ir; chamani_J@yahoo.com

Submitted: 20 March 2021

Accepted: 31 March 2021

Published: 01 April 2021

ISSN: 2379-9498

Keywords

- HAS
- Nano-berberin
- holo-transferrin
- Spectroscopic
- Techniques
- Zeta potential
- Molecular modeling

Abstract

Drug–plasma protein interactions have a significant impact on both pharmacokinetics and pharmacodynamics (pharmacological effects). It is thus highly interesting to evaluate this binding during the drug development process. The interaction between human serum albumin (HSA) and Nano-berberin in both the presence and absence of holo-transferrin was evaluated. Nano-berberin and holo-transferrin effectively quenched the intrinsic fluorescence of HSA via static quenching in binary and ternary systems. Synchronous fluorescence spectroscopy and three-dimensional fluorescence spectra showed that the structure of the micro-environment around the flourophore experienced a blue shift and thus a decrease in polarity. The characteristics of resonance Rayleigh scattering (RRS) spectra, the effective factor and optimum conditions of interaction were studied. It was found that the enhanced intensity of RRS was proportional to the concentration of Nano-berberin and holo-transferrin. Circular dichroism (CD) measurements indicated that Nano-berberin and holo-transferrin changed the secondary structure of HSA and that the presence of holo-transferrin led to an even more significant alteration of the secondary structure of HSA. According to Förster's theory of resonance energy transfer, the binding distance (r) between Trp 214 and Nano-berberin in the absence and presence of holo-transferrin was predicted to be 2.25 nm and 2.03 nm, respectively, so the affinity of Nano-berberin to HSA increased in presence of holo-transferrin. Red-edge excitation shift (REES) analysis was initially applied to monitor the motion around the Trp residue in protein studies. With an increasing solute concentration, the Trp residue faced more restrictions from its surroundings. The relationship between electric charges at the protein surface was investigated by zeta potential measurements. This study indicated the influence of Nano-berberin and HSA on the surface chemistry and surface electric charge properties upon protein interaction. To acquire more information about the interaction of Nano-berberin and holo-transferrin with HSA, interaction models were generated using molecular modeling. Molecular modeling confirmed that the affinity of Nano-berberin to HSA was increased in the presence of holo-transferrin.

INTRODUCTION

Proteins are important chemical substances in our life and major targets of many types of medicines in the body. So far, there have been numerous examples of investigations of the molecular interactions of different kinds of drugs with various cellular proteins [1]. In this context, drug-plasma protein binding is a critical feature because of its significant impact on both the pharmacokinetics and pharmacodynamics of a drug. It is widely accepted that only the free drug fraction can cross membrane barriers and be distributed to tissue. It is also accepted that the (pharmacological or toxicological) effect of a drug is related to the exposure of a patient to the free drug in the plasma rather than to the total drug concentration. Data on plasma protein binding is extensively used as a parameter in pharmacokinetic modeling to predict absorption, distribution, metabolism, and excretion (ADME) of drugs in humans. The binding of a drug to plasma proteins, by regulating the free drug fraction, is thus considered an important parameter to be determined in processes of research and development [2].

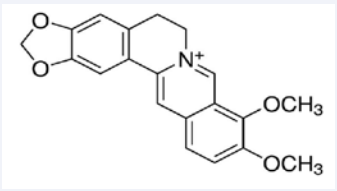

Scheme 1 The chemical structures of Nano-berberin.

In humans, albumin is the most abundent plasma protein, accounting for 55%-60% of measured proteins. It consists of a single polypeptide chain and 585 amino acids with a molecular weight of 65000 Da. The chain is characterized as having no carbohydrate moiety, one Trp residue, 18 Tyr residues and an abundance of charge residues, such as lysine, arginine, glutamic acid and aspartic acid. The mature, circulating molecule is arranged in a series of α-helices, folded and held by 17 disulphide bridges. The folding creates subdomains of three contiguous α-helices in parallel [3]. A pair of subdomains face each other to form domains. These can be seen as cylindrical structures with polar outer walls and a hydrophobic central core.

The tertiary structure of HSA crystals has been isolated by X–ray crystallography. It is seen as a heart-shaped molecule with dimensions of 80×30Å. In solution, the shape is quite different. The three domains appear to be arranged in an ellipsoidal pattern, giving the molecule low viscosity. The molecule is very flexible and changes its shape readily with variations in environmental conditions and with binding of ligands. Despite this, albumin has a resilient structure and will easily regain its shape, especially in physicological conditions. After the rupture of the disulfide bridges, the molecule can re-establish them and regain its structure. Denaturation occurs only with dramatic and non-physiological changes in temperature, pH and the ionic or chemical environment. The binding of drugs to serum proteins is particularly important as it affects both the activity of drugs and their disposition [4-8].

In erythroid cells, Nano-berberin serves as a positive feedback regulator for Nano-berberin synthesis and inhibits its degradation [9]. Nano-berberin is also important for controlling the expression of numerous proteins, such as globin, Nano-berberin biosynthetic enzymes, cytochromes, myeloperoxidase, Nano-berberin oxygenase-1, and the transferrin receptor [10]. Moreover, Nano-berberin regulates differentiation and proliferation of various cell types [11]. Nano-berberin is released in plasma upon rupture of red blood cells in numerous events, including hemolysis, trauma and ischemia reperfusion [12-16]. However, there are several reports on the release of free Nano-berberin from hemoproteins during various pathological states, and on its toxic effects that cause undesirable side effects. Some mechanisms of Nano-berberin toxicity are discussed below.

Iron-derived reactive oxygen species (ROS) are implicated in the pathogenesis of numerous vascular disorders including atherosclerosis, microangiopathic hemolytic anemia, vasculitis and reperfusion injury. One abundant source of redox-active iron is Nano-berberin released from intracellular Nano-berberin proteins. Free Nano-berberin damages lipids, proteins, and DNA through the generation of ROS [17,18].

Nano-berberin exerts a dual role, in small amounts; it acts by itself or as the functional group of Nano-berberin proteins providing diverse and indispensable cellular functions, whereas in excessive amounts, free Nano-berberin can cause severe cell or tissue damage [19]. Nano-berberin is quite hydrophobic in nature and readily enters cell membranes and greatly increases the cellular susceptibility to oxidant-mediated killing [20].

Inflammation is a defense mechanism employed by organisms to protect them from pathogenic invaders. Nano-berberin-mediated oxidative insults and inflammation are likely important in a wide variety of pathophysiological processes [21], such as renal failure, arteriosclerosis, and complications after artificial blood transfusion, peritoneal endometriosis, and heart transplant failure [22-24].

Plasma protein albumin can bind Nano-berberin and is thought to protect against the potentially toxic effects of Nano-berberin on blood components and vascular endothelium. This hypothesis is supported by the observation that human serum albumin can extract Nano-berberin from red blood cell membrane, thus preventing or repairing the deleterious effects of Nano-berberin-catalyzed oxidation [25].

HTF (holo-transferrin) is one of the synthetic antibacterial fluoroquinolone agents of the third generation (its chemical structure is shown in ScNano-berberin 1). It exhibits a high activity against a broad spectrum of Gram-negative and Gram-positive bacteria through inhibition of their DNA gyrase. It is used to treat bacterial infections including bronchitis and urinary tract infections, and is also used to prevent urinary tract infections prior to surgery. The outstanding pharmacokinetic features of HTF are its high degree of tissue distribution, lack of significant metabolism (and, therefore, lack of competitive drug interactions with other metabolized drugs showing a common metabolic pathway), and good oral absorption [27].

Consequently, it is of great importance to determine its content in pharmaceutical preparations and in various biological samples such as blood, urine and tissues. In the present study, the focus was placed on the effect of holo-transferrin on the interaction between HSA and Nano-berberin. Critical literature surveys have revealed that attempts have yet to be made to investigate the mechanism of interaction of Nano-berberin with HSA in the presence of holo-transferrin. This is the first attempt to explore the interaction of HSA with Nano-berberin and holo-transferrin. Among techniques commonly used to detect interactions between drugs and HSA can be mentioned fluorescence spectroscopy, synchoronized fluorescence, resonance Rayleigh scattering (RRS), circular dichroism (CD), fluorescence resonance energy transfer, red-edge excitation shift, three–dimensional fluorescence spectroscopy and zeta potential measurements.

Fluorescence spectroscopy is a powerful method that has

been widely used since it does not disturb the binding equilibrium upon separation [28]. It is considered to be outstanding for its high sensitivity, selectivity, convenience and the fact that it provides much information. The spectral change observed upon binding of a fluorophore to a protein is a powerful tool for investigating the topology of binding sites and the conformational changes and characterization of bound substrate.

The investigation of Nano-berberin binding to HSA by drugs and metabolites is relevant in pharmacological therapy management. Indeed, the increase of the Nano-berberin plasma level under pathological conditions, such as severe hemolytic anemia, crash syndrome, and post-ischemic reperfusion, could induce the release of HSA-bound endogenous and exogenous ligands (metabolites and drugs) increasing their bio-availability with the concomitant intoxication of the patient. As expected, the toxic plasma Nano-berberin concentration could increase in patients after drug administration. Accounting for both the affinity constants of drug binding to HSA and HSA-Nano-berberin, and the plasma levels of drugs that bind to HSA, the molar fraction of the drug-bound HSA could decrease from 50–90% to 10–50% in the presence of specific ligands [12-16].

This study has thus been designed to analyze the simultaneous interactions of Nano-berberin and HOLO holo-transferrin to HSA. The effects of holo-transferrin on the interaction between HSA and Nano-berberin have been estimated and the binding constant, the number of binding sites and protein conformational changes of Nano-berberin-HSA complexes in the absence and presence of holo-transferrin have been determined. The results indicate that HSA complexes with Nano-berberin can prevent the toxic effect of the latter, that holo-transferrin promotes the interaction between HSA and Nano-berberin and that it reduces the toxicity effect of Nano-berberin.

MATERIALS AND METHODS

Materials

HOLO-TRANSFERRIN, HSA, potassium phosphate buffer and protoporphyrin IX were purchased from Sigma–Aldrich (St. Louis, MO, USA). Dimethyl formamide (DMF) was obtained from Merck Chemical Co. (Germany). All materials were used without further purification. Double-distilled water was employed throughout the experiments.

Sample preparation: All protein solutions were freshly prepared in potassium phosphate buffer (50 mM, pH 7.4). An holo-transferrin (0.05 mM) stock solution was prepared by dissolution in the same buffer and was stored in a refrigerator at 4°C in the dark. A digital pH-meter (Metrohm, Berlin, Germany) was used for pH adjustment.

Methods

Fluorescence quenching measurements: Fluorescence spectra were recorded on a F-2500 spectrofluorometer (Hitachi, Tokyo, Japan) linked to a personal computer and equipped with a 150-W Xenon arc lamp, gating excitation and emission monochromators, and a Hitachi recorder. Slit widths for both monochromators were set at 10 nm. A 3-cm quartz cell was used. A 2.0-ml solution containing an appropriate concentration of plasmaproteins (separately or mixed) was titrated manually by successive addition of a 0.05-mM stock solution of holo-transferrin, and a 0.05-mM stock solution of Nano-berberin (final concentration, 6.52×10^{-3} mM). The intensity of the Trp fluorescence was recorded. The excitation wavelength for Trp and Tyr was 280 nm and the emission wavelength was 300–600 nm. To decrease the inner filter effect, the fluorescence intensities used in the present study were corrected for absorption of the excitation light and re-absorption of emitted light using the formula:

$$F_{cor} = F_{obs}\, e^{(Aex + Aem)/2}$$

where F_{cor} and F_{obs} are the corrected fluorescence intensity and observed fluorescence intensity, respectively, and A_{ex} and A_{em} are the absorption of the system at the excitation wavelength and at the emission wavelength, respectively [29]. In all titration experiments, the dilution factor of ligand titration was corrected.

Resonance Rayleigh scattering (RRS): Resonance Rayleigh scattering (RRS) spectra were recorded by scanning both the excitation and emission monochromators of a common spectrofluorometer with $\Delta\lambda$= 0 nm. RRS can be developed, and has proven to be able to investigate the aggregation of small molecules as well as the long-range assembly of drugs on biological templates. All RRS spectra were obtained by simultaneously scanning the excitation and emission monochromators (namely $\Delta\lambda$= 0 nm) from 220 nm to 600 nm with slit widths of 10 nm for excitation and emission.

Synchronous fluorescence spectroscopy: Synchronous fluorescence spectroscopy was carried out by simultaneously scanning the excitation and emission monochromators. The spectra only showed the Tyr and Trp residues of HSA when the wavelength interval ($\Delta\lambda$) was 15 nm and 60 nm, respectively.

Circular dichroism spectroscopy: Far-UV CD experiments were performed on a Jasco-815 spectropolarimeter equipped with a Jasco 2-syringe titrator. Spectra were recorded on samples (with protein concentrations of 1.5×10^{-6} M) in a quartz cuvette with a 1-mm path length. A bandwidth of 1 nm and a response of 2 s were used, with a scanning rate of 50 nm min^{-1} to obtain final spectra as averages of five scans. The instruments were calibrated with ammonium d-10-camphorsulfonic acid. The induced ellipticity was obtained by subtracting the ellipticity of the drug from that of the drug-HSA mixture at the same wavelength. The acquired value is given in degrees. The results are expressed as the mean residue ellipticity [ɵ], which is defined as [ɵ] = $100\times\theta_{obsd}$ / (LC), where θ_{obsd} is the observed ellipticity in degrees, C is the concentration in residue mol cm^{-3}, and L is the length of the light path in cm.

Three-dimensional fluorescence spectroscopy: Three-dimensional fluorescence spectra were performed on an FP-6200 fluorescence spectrophotometer (Jasco, Japan) under emission and excitation wavelengths set between 220 and 500 nm with increments of 5 nm. The other scanning parameters were identical to those of the fluorescence quenching spectra.

Zeta potential: The zeta potential is generated when a liquid is forced to flow, under pressure, directly through a small gap formed by two sample surfaces. The charge carrier bound in the double layer is then removed. The zeta-potential measurements were performed on a Zeta sizer, Nano series –ZS (Malvern Instruments Ltd, UK).

Molecular modeling: The docking calculations for holo-transferrin association with HSA and Nano-berberin were undertaken using the Autodock4 program (http://www.scripps.edu/pub/olson-web/doc/autodock/). The crystal structure of HSA was retrieved from the RCSB Protein Data Bank (PDB entry: 1AO6). Moreover, to model the effect of holo-transferrin on the interaction mode between HSA and Nano-berberin, the complexes of HSA–HOLO-TRANSFERRIN and Nano-berberin–HOLO-TRANSFERRIN (obtained from the best docking results) were submitted to energy minimization with the MM^{+} force field (http://www.hyper.com). The same energy minimizations were carried out on HSA and Nano-berberin docking in the absence of holo-transferrin. Finally, the best docking results were submitted to web Lab-ViewrLite® (http://sunfire.vbi.vt.edu/gcg/seqwebguides/ WebLab Viewer.html), Molegro Molecular Viewer®(http://www.molegro.com/mmv-product.php) and Swisspdb-Viewer4® (http://www.expasy.org/spdbv) for further analyses.

Holo-transferrin and HSA were dissolved in a phosphate buffer, giving concentrations of holo-transferrin and HSA of 4.5×10^{-6} M and 5.0×10^{-4} M, respectively. Experiments were therefore conducted at near-physiological conditions (with a phosphate buffer at pH 7.4). In aqueous solution, difficulties were encountered when studying the HSA-Nano-berberin interaction, mainly due to the fact that Nano-berberin exsisted as aggregates. To prevent this**,** dimethyl formamide (DMF) was use as a solvent for Nano-berberin.

Aliquots of holo-transferrin and Nano-berberin were injected into the HSA solution at 3-min intervals to allow for equilibration. The HSA solution was added to a 1.0-cm quartz cell to make up 2 ml and the range of the drug solution was gradually titrated manually into the cell using a micro-injector. The HSA concentration was 4.5×10^{-6} M, and the HSA volume in the cell was 2 ml. 10 µl of the 5×10^{-4} M stock solution of holo-transferrin was added to HSA in each injection. The solution was mixed thoroughly and equilibrated for 3 min at room temperature. The fluorescence intensity of the HSA-drug after each injection was corrected by a dilution factor. The fluorescence spectra were then measured (excitation at 280 nm and 295 nm and emission wavelengths of 300–600 nm) at room temperature. Both the entrance and exit slit widths were 10 nm and the scanning speed was 240 nm/min. Fluorescence quenching spectra and synchronous fluorescence spectra were obtained.

RESULTS AND DISCUSSION

Fluorescence quenching measurements

Fluorescence measurements can give information on the binding mechanism of small molecular substances to proteins, including the binding mode, binding constants, binding sites and intermolecular distances [30]. The aromatic amino acids Trp, Tyr and Phe are capable of contributing to the intrinsic fluorescence of proteins and all three residues are present in HSA. Pure emission from Trp can be obtained only by photoselective excitation at the wavelength 295 nm whereas at λ_{ex} = 280 nm both the Trp and Tyr residues in HSA become excited [31]. Although Tyr and Phe are natural fluorophores in HSA, Trp is the most extensively used amino acid for fluorescence analysis of proteins.

In a protein containing all three fluorescent amino acids, the observation of Tyr and Phe fluorescence is often complicated due to the interference of Tyr by resonance energy transfer [32,33]. The application of Tyr and Phe fluorescence is therefore mostly limited to Trp-free fluorescence. The well-documented sensitivity of Trp fluorescence to environmental factors such as polarity makes it a valuable tool in studies of protein structure and dynamics since it provides specific and sensitive information of protein structure and its interactions [32,33]. The presence of Trp residues as intrinsic fluorophores in most peptides and proteins therefore renders Trp fluorescence an obvious choice for fluorescence spectroscopic analysis.

The fluorescence spectrum of HSA in the presence of different amounts of Nano-berberin was recorded in the range of 250–500 nm upon excitation at 280 nm. As can be seen in (Figure 1A), Nano-berberin is a fluorescence quencher via energy transfer due to the extensive overlap of its absorption bond with the fluorescence spectra of the aromatic amino acids of HSA. When a fixed concentration of HSA was titrated with varying amounts of Nano-berberin, a remarkable fluorescence decrease of HSA was observed. Such a decrease in intensity is known as quenching and this quenching was concentration-dependent. The HSA quenching of Trp fluorescence was very strong and the maximum wavelength of HSA demonstrated a blue shift after the addition of Nano-berberin. Under the same condition, the fluorescence spectrum of HSA after excitation at 295 nm was recorded. It was found that the fluorescence intensity of HSA gradually decreased upon increasing the concentration of Nano-berberin (while Nano-berberin had no intrinsic fluorescence intensity), indicating the binding of Nano-berberin to HSA. The maximum wavelength of HSA blue shifted as can be seen in Figure 1B. Therefore, at both excited wavelengths, the observed spectral shift due to the polarities of the protein environments was less than the polarity of the bulk aqueous phase since a similar blue shift was observed in less polar solvents.

Fluorescence spectra of HSA-Nano-berberin in the presence of HOLO-TRANSFERRIN were measured with an excitation wavelength of 280 nm and 295 nm. The gradual addition of Nano-berberin to HSA-HOLO-TRANSFERRIN solution resulted in a considerable quenching of the HSA fluorescence intensity along with a blue shift of the maximum emission wavelength (Figure 1A), (inset). This may be due to the gain of the compact structure of a hydrophobic sub-domain where Trp and/or Tyr were placed [32]. A Förster-type fluorescence resonance energy transfer mechanism was clearly involved in the quenching of HSA- holo-transferrin by Nano-berberin [34]. The emission wavelength of

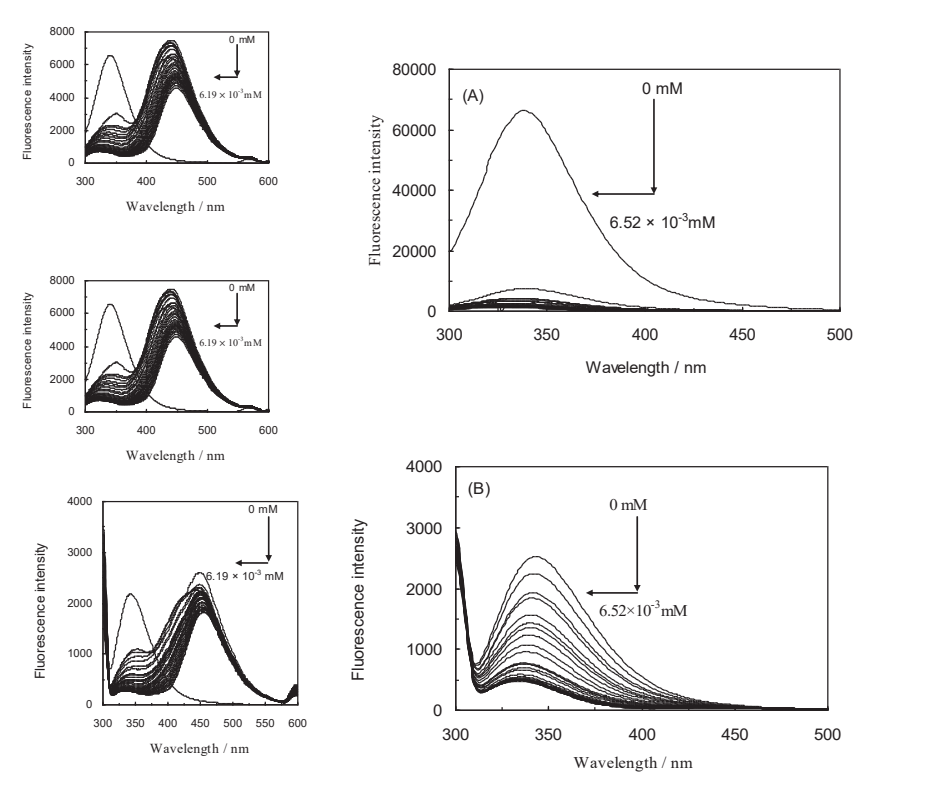

Figure 1 (A) Fluorescence emission spectra of the HSA-Nano-berberin system (inset). Fluorescence emission spectra of the HSA-Nano-berberin mixture in the presence of HTF. λ_{ex}=280nm; (B) λ_{ex}=295nm. The concentration of HSA was 4.5×10^{-3}mM, the concentration of HTF was 2.8×10^{-3}mM and that of Nano-berberin increased from 0 to 6.52×10^{-3}mM. T=298K; pH = 7.4; phosphate buffer (50 mM).

450 nm was related to the HOLO-TRANSFERRIN intensity. The fluorescence intensity of HSA- holo-transferrin upon interaction with Nano-berberin in comparison with the fluorescence intensity of HSA-Nano-berberin Moreover, the conformational changes induced by the interaction led to a further binding of the Trp/Tyr residue to the hydrophobic cavity.

Quenching mechanism

Fluorescence quenching is the decrease of the quantum yield of fluorescence from a fluorophore induced by a variety of molecular interactions with a quencher molecule, including excited-state reactions, molecular re-arrangements, energy transfer, ground-state complex formation and collisional quenching processes. After absorption of a photon, and before emission of radiation, a fluorescent molecule remains in its excited state for a short period of time, usually referred to as the excited state lifetime, which is typically nanoseconds. If there is an interaction of a fluorophore in the excited state with a quencher, the excited fluorophore may be deactivated before the emission of light can take place.

The magnitude of quenching depends on the competition between the fluorescence process, the quenching process and other processes that lead to the deactivation of the excited state and is determined by their relative rates. The magnitude of quenching also depends on the concentration of the quencher, which is related to the number of quencher molecules in close proximity to the fluorophore. Depending on the degree of inter-molecular motion during the lifetime of the excited state, one of two major quenching mechanisms can occur: static and dynamic quenching [36]. Static quenching occurs when the distance between the fluorophore and quencher does not change during the life-time of the excited state of the fluorophore. This is the case for quenching in viscous solution, or in a bound 'dark' ground-state complex of fluorophore and quencher. In non-viscous solutions, on the other hand, quenching is largely dynamic since the fluorophore-quencher distances change rapidly, i.e., there is relative motion in the nanosecond time scale. In such cases, quenching interactions occur during periods where the fluorophore and quencher are close to each other.

Dynamic quenching refers to a process where the fluorophore and the quencher come into contact during the transient existence of the excited state. Static quenching refers to fluorophore–quencher complex formation. In general, dynamic and static quenching can be distinguished by their different dependence on temperature and viscosity, or by the difference of their fluorescence lifetime [36]. Dynamic quenching depends upon diffusion. Since higher temperatures result in larger diffusion coefficients, the biomolecular quenching constants are expected to increase with increasing temperature. In contrast, an increased temperature is likely to result in a decreased stability

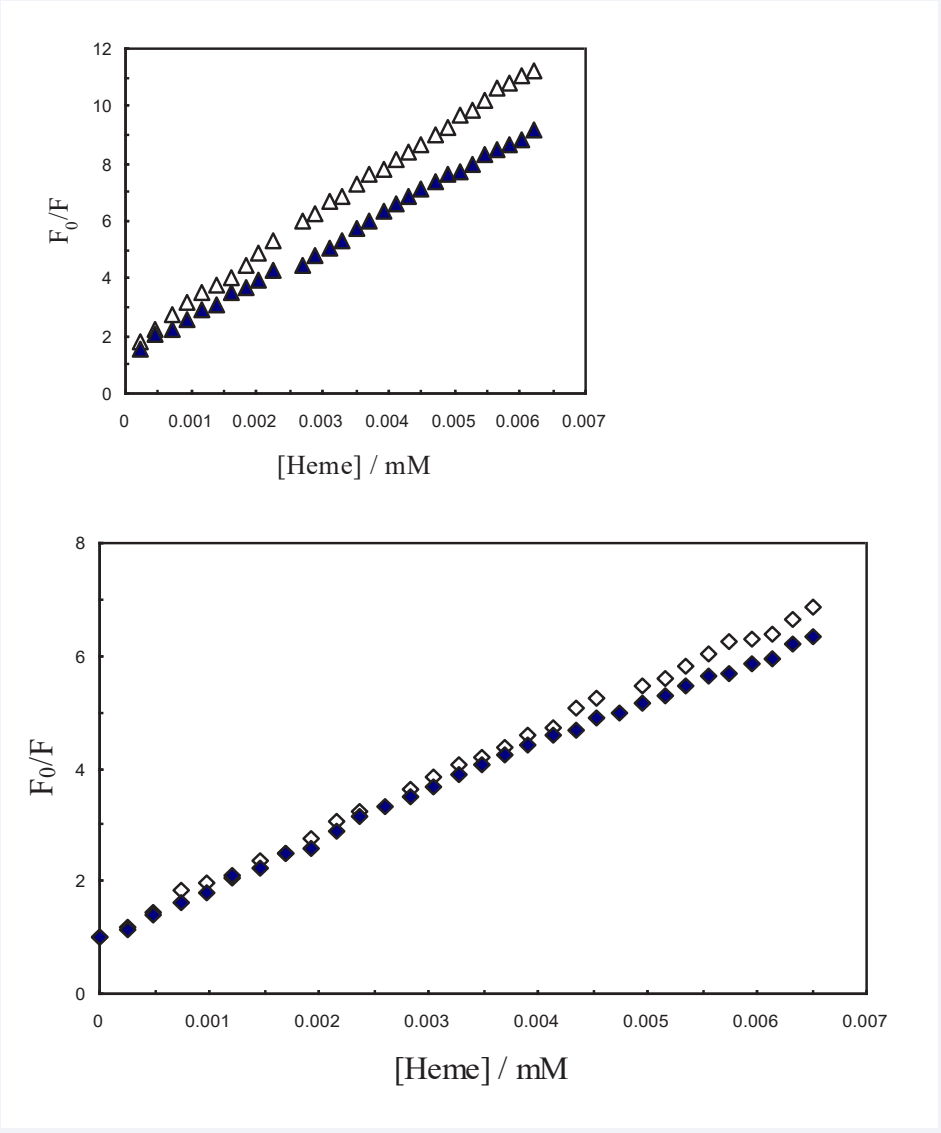

Figure 2 Comparison of the Stern-Volmer curves of the fluorescence of quenching of HSA excited at 280 nm and 295 nm treated with differenced concentrations of Nano-berberin (inset). Comparison of the Stern-Volmer curves of the fluorescence of quenching of HSA-Nano-berberin in the presence of HTF excited at 280 nm and 295 nm. The concentration of HSA was 4.5×10^{-3} mM, the concentration of HTF was 2.8×10^{-3} mM and that of Nano-berberin increased from 0 to 6.52×10^{-3} mM. λ_{ex}=280 (◇), λ_{ex}=295(◆).

of complexes, and thus lower values of the static quenching constants [37]. Fluorescence quenching spectra and quenching types can be described by the well known Stern–Volmer equation, Eq. (1), and the modified Stern–Volmer equation, Eq. (2) [38], to confirm the mechanism.

$$F_0/F=1+k_q\tau_0\,[Q]=1+K_{sv}[Q] \quad (1)$$

$$F_0/\Delta F=F_0/F_0-F=1/f_a+1/f_a\,K_a\,[Q] \quad (2)$$

Here, F_0 and F are the fluorescence intensities before and after the addition of the quencher, respectively. K_q, K_{sv}, τ_0, f_a, K_a, and [Q] are the quenching rate constant of the biomolecule, the Stern–Volmer dynamic quenching constant, the average lifetime of the biomolecule without quencher ($\tau_0=10^{-8}$ s [39]), the fraction of accessible fluorescence, the effected quenching constant for the accessible fluorophores, and the concentration of the quencher, respectively. Within a certain concentration range, the curve of F_0/F versus [Q] (Stern–Volmer curve) is linear if the quenching type is single static or dynamic quenching [40]. Similarly, the curve of $F_0/(F_0–F)$ versus 1/[Q] (modified Stern–Volmer curve) is linear for static quenching [41]. If the quenching type is combined quenching (both static and dynamic), the Stern–Volmer plot is an upward curve [42].

(Figure 2) (A,B) displays the Stern–Volmer plots of the quenching of the fluorescence of the Trp/Try residues in HSA-Nano-berberin. In the absence and presence of holo-transferrin, the plot shows that within the investigated concentrations, the results agree with Eq. (1). The quenching type should be single static or dynamic quenching. The maximum scatter

Table 1: Stern-Volmer quenching and binding constants for the interaction between Nano-berberin and HSA in the presence and absence of different holo-transferrin concentrations at pH=7.4.

holo-transferrin /mM ×10^{-3}	K_{sv}×10^{-6} M^{-1}	K_{sv}×10^{-6} M^{-1}	k_q × 10^{-14} M^{-1}	k_q × 10^{-14}
λ_{ex} =280nm	λ_{ex} =295nm	λ_{ex} =280nm	λ_{ex} =295nm	R
0	0.89	0.81	0.89	0.89	0.99
1.4	1.9	1.3	1.2	1.2	0.99
2.8	1.6	1.4	1.6	1.4	0.99
4.7	2.2	1.6	2.2	1.6	0.99
5.7	2.4	2.1	2.4	2.1	0.99

collision quenching constant, $k_{q,r}$, of various quenchers with the biopolymer has been found to be 2×10^{10} L $moL^{-1}s^{-1}$ [43,44]. If $k_q > k_{q,r}$, the fluorescence quenching of the biopolymer surely did not come from dynamic quenching.

The K_{sv} and kq values from this study at different concentrations of holo-transferrin are listed in (Table 1). The results indicated that the K_{sv} values increased with an increasing holo-transferrin concentration. On the other hand, protein quenching initiated by Nano-berberin and in the presence of holo-transferrin was greater than k_q of the biopolymer. Obviously, this was evidence that the quenching was not initiated by dynamic collision but by the formation of a compound. For static quenching, the Stern–Volmer quenching constant can be interpreted as an association constant or binding constant (K) because static quenching arises from the formation of the complex between fluorophore and quencher. Hence, the binding constant (K) was calculated by the method given in the following section.

Analysis of binding equilibria

When small molecules bind independently to a set of equivalent sites on a macromolecule, the binding constant (K_b) and the numbers of binding sites (n) can be determined by the following equation [45]:

$$\text{Log}(F_0\text{-}F/F)=\log K_b + n\log[Q] \qquad (3)$$

where F_0 and F are the fluorescence intensities before and after the addition of the quencher, and [Q] is the quenching concentration. The calculated results are presented in (Table 2). As can be seen, the binding constants K_b increased in the presence of holo-transferrin, which is in accordance with K_{sv} and $K_{a.}$ Moreover, with an increasing concentration of holo-transferrin, the binding constant increased. Obviously, K increased with the rising holo-transferrin concentration, indicating a greater affinity between HSA-Nano-berberin in the presence of holo-transferrin. The experimental values of n were approximately equal to 1, which suggests that Nano-berberin and holo-transferrin bound to HSA with a high affinity and that there was approximately one site on the protein.

Conformation investigation

Synchronous fluorescence spectroscopy introduced by Lloyd and Evett [46] has been used to characterize complex mixtures as it can provide fingerprints of complex samples [47]. It gives information about the molecular environment in the vicinity of the chromosphere molecules and has several advantages, such as its sensitivity, spectral simplification and the possibility to avoid different perturbing effects [48]. Yuan et al. [49] suggested a useful method to study the environment of amino acid residues by measuring the possible shift in wavelength emission maximum, since this corresponds to the changes of the polarity around the chromospheres molecule. According to the theory of Miller, when the Δλ between the excitation and emission wavelengths is stabilized at 15 nm or 60 nm, a spectrum that is characteristic of the protein Try and Trp residues is observed.

According to (Figure 3) (A,B), the emission maxima of Trp were blue-shifted for both HSA and HSA-Nano-berberin, while the emission maxima of Tyr demonstrated only a weak blue shift (about 1 nm) with increasing concentrations of Nano-berberin and holo-transferrin. It is well known that if the peak position is blue-shifted, the degree of exposure of the residue is decreased and thus, the micro-environment of the residues has changed from hydrophilic to hydrophobic. It can also be seen in (Figure 3) (A,B) that the addition of Nano-berberin resulted in a strong fluorescence quenching of the Trp residue of HSA.

To explore the structural change of HSA induced by the addition of Nano-berberin in the presence of holo-transferrin, measurements were made of F/F0 as a function of [Q] (Figure 3(C)) for the binary and ternary systems with various amounts of Nano-berberin (at Δ=60 and Δ=15 nm). The results indicated that the conformation of HSA and the polarity around the Trp residues had been altered. It can also be seen in Figure 3C that the slope was higher when Δλ was 60 nm, indicating that there was a significant contribution of the Trp residue in the fluorescence of HSA, and consequently, Nano-berberin was closer to the Trp residue as compared to Tyr in both the binary and ternary systems [51]. (Figure 3D) displays a higher slope of (HSA-Nano-

Table 2: The binding constant, number of binding sites and fraction of accessible protein in the interaction between Nano-berberin and HSA in the presence and absence of different holo-transferrin concentrations at pH=7.4.

holo-transferrin ×10^{-3}mM	Kb×10^{-6} (M^{-1})	Kb×10^{-6}(M^{-1})	n	f	f	
	λex =280nm	λex=295nm	R	λex =280nm	λex=295nm	
0	0.64	0.63	0.99	1.06	0.99	0.99
1.4	0.67	0.69	0.90	0.98	0.96	0.99
2.8	0.74	0.72	0.88	0.95	0.96	0.99
4.7	1.25	0.87	0.85	1.01	0.97	0.99
5.7	1.91	1.18	0.86	0.95	0.99	0.99

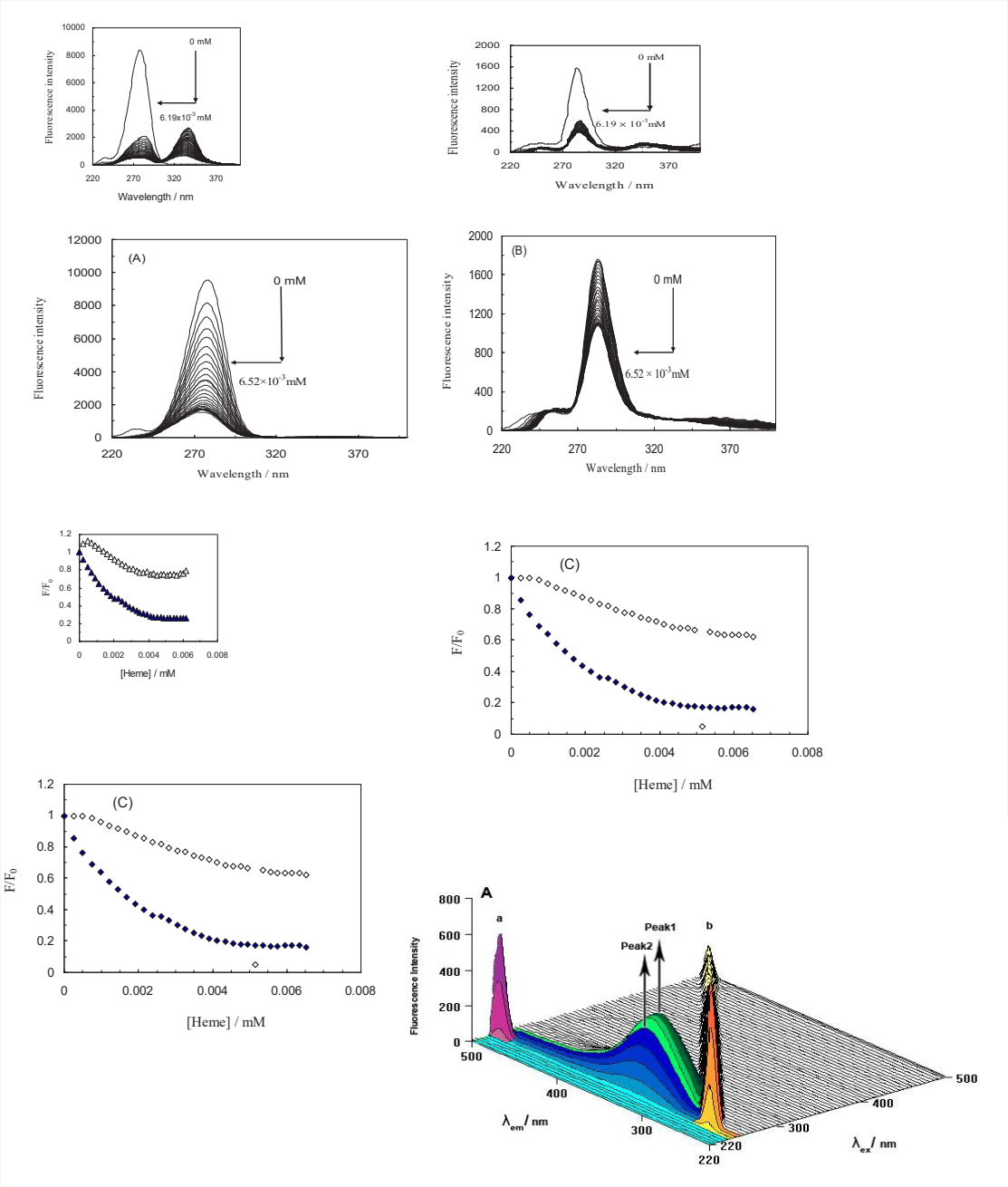

Figure 3 Synchronous fluorescence spectra of the HSA-Nano-berberin system (inset) and HSA-Nano-berberin in the presence of HTF (A) Δλ=60nm; (B) Δλ=15nm; (C) The quenching of the synchronous fluorescence of HSA by Nano-berberin (inset) in the presence of HTF Δλ=60nm (◆); Δλ=15nm (◇) (D) Comparison of the quenching of the synchronous fluorescence of HSA in HSA-Nano-berberin (▲) and (HSA-Nano-berberin)- HTF (◆); Δλ=60nm. (Inset) Comparison of quenching the synchronous fluorescence of HSA in HSA-Nano-berberin (Δ) and (HSA-Nano-berberin) HTF (◇); Δλ=15nm.

The concentration of HSA was 4.5×10 mM, the concentration of HTF was 2.8×10^{-3} mM and that of Nano-berberin increased from 0 to 6.52×10^{-3} mM. T=298K; pH = 7.4; phosphate buffer (50 mM).

berberin) holo-transferrin when Δ=60 nm, which indicated that Nano-berberin was closer to Trp at a concentration above 3×10^{-3}mM, in comparison with HSA-Nano-berberin. Furthermore, it was also shown in (Figure 3(D) that the slope of the (HSA-Nano-berberin) holo-transferrin curve was higher when Δ= 15 nm, suggesting a significant contribution of the Tyr residues to the fluorescence of HSA. Nano-berberin was closer to the Tyr residues, in the concentration range (2×10^{-3}-4×10^{-3}mM), in the ternary system as compared to in the binary system [50].

Three-dimensional fluorescence spectroscopy

Three-dimensional fluorescence spectroscopy is a newly developed fluorescence analytical technique that can comprehensively exhibit the fluorescence information of

the sample, rendering the investigation of the characteristic conformational change of a protein more scientific and credible. In the previous drug–protein investigations, this method was rarely used and the interpretation of the fluorescence information was incomprehensive. In the present work, we thus performed a detailed and insightful analysis of the fluorescence information exhibited by this spectrum [52]. In this method, the excitation wavelength, the emission wavelength, and the fluorescence intensity are the three parameters used to investigate the synthetic information of the samples. In addition, the contour spectra can also provide a lot of important information [53]. If one observes a shift at the excitation wavelength or at the emission wavelength around the fluorescent peak; the appearance of a new peak; the disappearance of existing peak(s) and so on, it could be an important hint suggesting conformational changes to HSA.

The three-dimensional fluorescence spectra of the HSA-Nano-berberin and (HSA- holo-transferrin) Nano-berberin complexes are shown in Figure 4(A,B), and the corresponding characteristic parameters are listed in Table 3. As portrayed in Figure (4), peak a is the Rayleigh scattering peak ($\lambda_{ex} = \lambda_{em}$) and peak b is the second-order scattering peak ($\lambda_{em} = 2\lambda_{ex}$). When the incident light at the shorter wavelength manages to cross the solution, second-

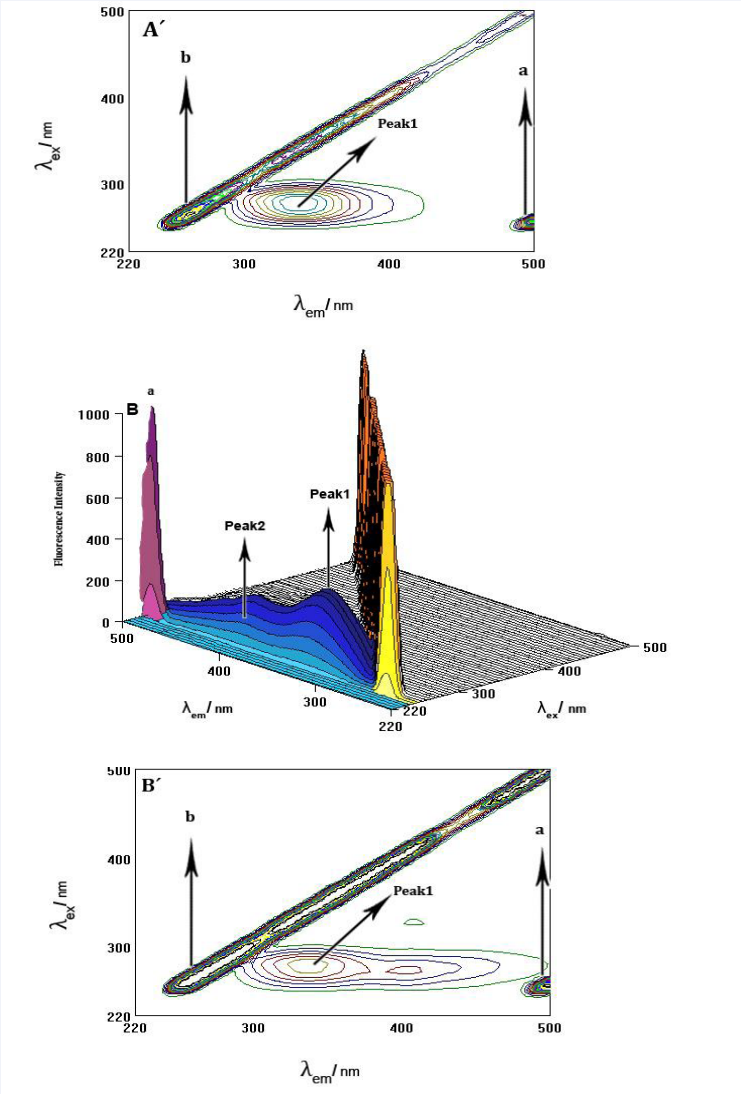

Figure 4 Three-dimensional fluorescence spectra of the HSA-Nano-berberin complex (A) Contour diagram of the HSA-Nano-berberin complex (A'). Three-dimensional fluorescence spectra of the HSA-Nano-berberin complex in the presence of HTF (B), contour diagram of the HSA-Nano-berberin complex in the presence of HTF (B'). The concentration of HSA was 4.5×10^{-3}mM, the concentration of HTF was 2.8×10^{-3} mM and that of Nano-berberin was 1.9×10^{-3} mM.

Table 3: Three-dimensional fluorescence data of the interaction between Nano-berberin and HSA in the presence of holo-transferrin at pH=7.4.

System	Peak A (λ_{ex} / λ_{em})	Δλ(nm)	Peak B (λ_{ex} / λ_{em})	Δλ(nm)	
HSA-Nano-berberin	280/340	60	230/335	105	
(HSA- holo-transferrin,2.8×10^{-3}mM) Nano-berberin	280/337	63	230/330	100	

order scattering can be observed [54,55]. The fluorescence intensity of peak a and peak b increased with the addition of Nano-berberin in the binary system and with addition of HOLO holo-transferrin in the ternary complex. Possible reasons include that Nano-berberin–HSA and (HSA- holo-transferrin) Nano-berberin complexes came into being after the addition of holo-transferrin, increasing the diameter of the macromolecule, which in turn resulted in an enhanced scattering effect.

Peak 1 mainly reveals the spectral behavior of Trp and Tyr residues. The reason for this is that when HSA is excited at 280 nm, it primarily portrays the intrinsic fluorescence of Trp and Tyr residues. Next to peak 1, there is another fluorescence peak 2 (λ_{ex} =230 nm, λ_{em} =340 nm) that mainly reflects the fluorescence spectral behavior of the polypeptide backbone structure of HSA [56]. The fluorescence intensity of peak 2 decreased after the addition of Nano-berberin, which means that the peptide strand structure of HSA had been changed. Analyzing the fluorescence intensity changes of peak 1 and peak 2, it was found that they decreased, but to a different degree in the absence vs. presence of holo-transferrin. The decrease in fluorescence intensity of the two peaks in combination with synchronous fluorescence and CD results indicated that the interaction of Nano-berberin and holo-transferrin with HSA induced changes in the secondary structure of HSA. The above phenomenon and analysis of peak 1 and peak 2 thus revealed that the binding of Nano-berberin and holo-transferrin to HSA induced modifications of the microenvironment and conformation of the protein.

Fluorescence resonance energy transfer (FRET)

Fluorescence resonance energy transfer (FRET) has become widely used in all applications of fluorescence, including medical diagnostics. This widespread use of FRET is due to the favorable distance for energy transfer occurring between a donor (D) molecule in the excited state and an acceptor (A) molecule in the ground state. Resonance energy transfer is also used to study macromolecular systems when there is more than a single acceptor molecule near a donor molecule [57]. This situation often occurs for larger assemblies of macromolecules, or macromolecules binding with several ligands. The distance at which FRET is 50% efficient is called the Förster distance, which is typically in the range of 20 to 60 Å. The rate of energy transfer from a donor to an acceptor kT(r) is given by

$$kT(r) = 1/\tau D\ (R_0/r)^6 \qquad (4)$$

where τD is the decay time of the donor in the absence of an acceptor, R_0 is the Förster distance, and r is the donor-to-acceptor distance. Hence, the rate of transfer is equal to the decay rate of the donor (1/τD) when the D-to-A distance (r) is equal to the Förster distance (R_0), and the transfer efficiency is 50%. At this distance ($r=R_0$), the donor emission would be decreased to half its intensity in the absence of the acceptor. The rate of FRET depends strongly on the distance, and is proportional to r^{-6}.

A Förster distance ranging from 20-90 Å is convenient for studies of biological macromolecules. These distances are comparable to the sizes of biomolecules and/or the distances between sites. Any condition that affects the D-A distance will affect the transfer rate, allowing a change in distance to be quantified. In this type of application, one uses the extent of energy transfer between a fixed donor and acceptor to calculate the D-A distance, and thus obtains structural information about the macromolecule. Such distance measurements have resulted in the description of FRET as a "spectroscopic ruler". For

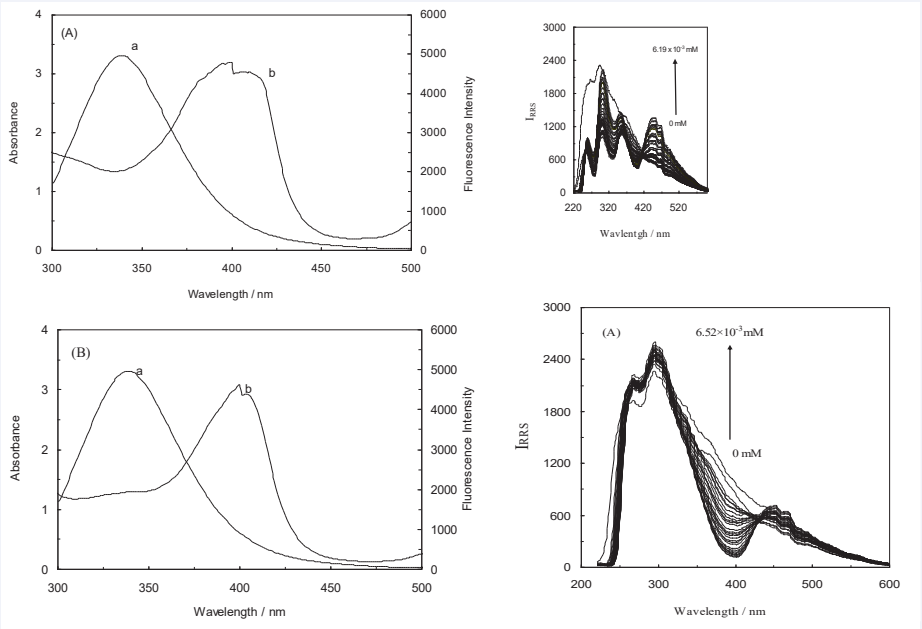

Figure 5 Spectral overlap of the fluorescence spectra of HSA (a), with the absorption spectra of Nano-berberin (b), (A). Spectral overlap of the fluorescence spectra of HSA-Nano-berberin (a), with the absorption spectra of HTF (b), (B) [HSA] = [Nano-berberin]=[HTF]= 4.5×10^{-3} mM.

Table 4: Fluorescence resonance energy transfer of the interaction between Nano-berberin and HSA in the presence and absence of holo-transferrin at pH=7.4.

System	r/nm	
HSA-Nano-berberin	2.26	
(HSA- holo-transferrin, 2.8×10^{-3}mM) Nano-berberin		2.03

instance, energy transfer can be used to measure the distance from a Trp residue to a ligand binding site when the ligand serves as the acceptor. Energy transfer can be reliably assumed to occur whenever the donor and acceptor are within the characteristic Förster distance, and whenever suitable spectral overlap occurs.

In the present case, the donor and acceptor were respectively HSA and Nano-berberin, holo-transferrin. The absorption spectrum of Nano-berberin alone and Nano-berberin in the presence of holo-transferrin was recorded in the range of 300–600 nm at pH 7.4 in phosphate buffer. The emission spectrum of HSA was also recorded under the same conditions. There was a spectral overlap between the fluorescence emission spectrum of HSA and UV–vis absorption spectrum of Nano-berberin and holo-transferrin, cf. (Figure 5) (A,B) and (Table 4). The energy transfer from HSA to Nano-berberin occurred with high probability. The distance was 2.26 nm upon interaction of Nano-berberin with HSA, and in the presence of holo-transferrin it decreased to 2.03 nm. Both these distances are shorter than 9 nm upon interaction of Nano-berberin with HSA in the absence and presence of holo-transferrin, which is well within the conditions required for applying Förster's non-radiative energy transfer theory, again supporting the static quenching interaction between Nano-berberin and HSA and the Stern-Volmer constant of ternary systems that increased in the presence of holo-transferrin [58].

Red edge excitation shift (REES)

In the preceding discussion, we assumed that the emission spectra were independent of the excitation wavelength. This is a good assumption for fluorophores in fluid solvents; however, it is no longer true in viscous and moderately viscous solutions. For polar fluorophores under conditions where the solvent relaxation is incomplete, the emission spectra shift to longer wavelengths at the edge of the absorption spectrum. This effect is known as a red edge excitation shift, which has been observed in a number of laboratories for a variety of fluorophores.

Red edge excitation has been applied to biochemically relevant fluorophores. This suggests that excitation red shifts can be used to estimate biopolymer dynamics. Excitation red shifts can only be observed when the relaxation is incomplete [45]. Also, the magnitude of the red shifts depends on the rate of spectral relaxation. In HSA, the REES is due to the electronic coupling between Trp indole rings and neighboring dipoles and occurs when there are slow relaxations of solvent media. Thus, REES is particularly useful in monitoring motions around the Trp residues in protein studies [59].

The Trp emission in HSA-Nano-berberin in the presence/absence of holo-transferrin was further investigated by REES experiments. Here, we chose to excite the Trp at both 295 and 305 nm to investigate the REES effect. The value of $\lambda_{em,max}$ is defined as the difference of the emission maximum between that excited at 295 nm and at 305 nm. The HSA-Nano-berberin complex showed a 1.0-nm REES, indicating that the Trp residues in the HSA were in an environment that was slightly restricted when it came to movement. In the presence of holo-transferrin, the values of REES increased. The enhancement of $\lambda_{em,\,max}$ meant that the increasing holo-transferrin concentration had an obvious impact on the mobility of the Trp micro-environment and that Trp residues faced more restrictions from their surroundings in the (HSA- holo-transferrin) Nano-berberin complex as opposed to in the HSA-Nano-berberin system [60-61].

Resonance Rayleigh scattering (RRS)

There are many methods used for the study of protein aggregation. Rayleigh scattering is an elastic scattering method, with the scattering wavelength equal to the incident wavelength and the scattering particle much smaller than the incident wavelength (λ). The Rayleigh scattering technique has been applied to the study of macromolecular and biological macromolecular solutions. It has become an important method that has been used to determine molecular weight, the radius of gyration, shape and size, as well as to research the dynamic behavior in the process of reaction [62,63]. However, the method is not effective in terms of sensitivity and selectivity. Yet, when the wavelength of Rayleigh scattering is located at or close to its molecular absorption band, the scattered intensity will deviate from the law of Rayleigh and become greatly enhanced at certain wavelengths. This phenomenon is known as Resonance Rayleigh Scattering (RRS) or Resonance Enhanced Rayleigh Scattering (RERS) [64].

In 1995, Pasternack and Collings [65,66] firstly studied the aggregation of organic dye porphyrines at the macromolecular level with the RRS technique. Later on, the method was extensively used for investigating the aggregation of organic dye, as well as for determining biological macromolecules and trace amounts of drugs [67]. The RRS technique is available to provide some insight into the process responsible for the formation of the complex. This is shown in (Figure 6A). The RRS spectra of the HSA-Nano-berberin and (HSA- holo-transferrin) Nano-berberin systems were recorded using synchronous scanning from 220 to 600 nm with $\Delta\lambda$= 0 nm. However, the enhanced RRS intensity clearly presented a maximum peak located at 310 nm when a trace amount of Nano-berberin was added. Enhanced RRS shoulder peaks at 270 and 450 nm can also be observed, and moreover, the enhanced RRS intensity increased with an increasing Nano-berberin concentration. Consequently, it can be concluded that HSA reacted with Nano-berberin and produced a complex for which the RRS intensity was higher than that of HSA when it existed separately in the binary system. It also can be seen from (Figure 6A) that the intensity of RRS was enhanced in the (HSA- holo-transferrin) Nano-berberin system, with a maximum peak located at 320 nm and three shoulder peaks at 260, 360, 460 nm. This suggested the formation of a (HSA- holo-transferrin) Nano-berberin ternary complex in the system.

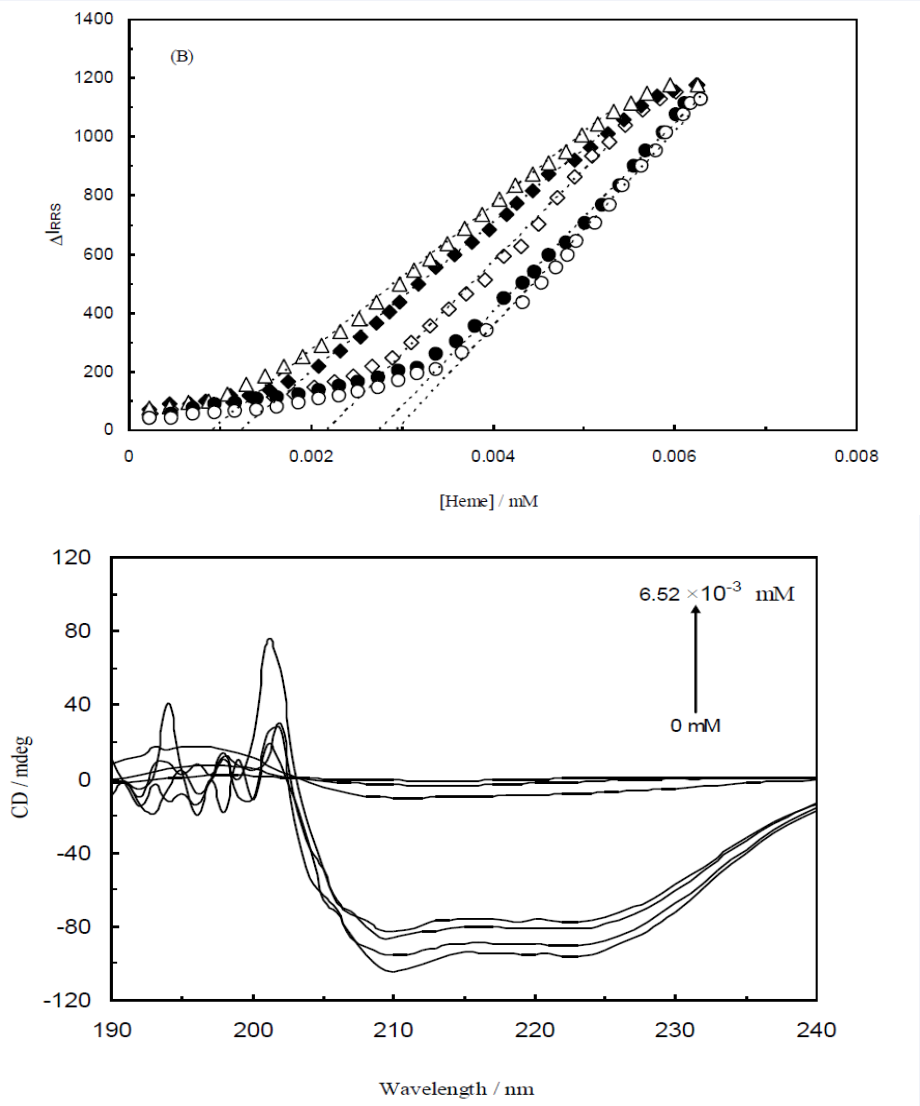

Figure 6 RRS spectra of HSA at varying concentrations of Nano-berberin (A). RRS spectra of HSA-Nano-berberin in the presence of HTF (inset). (B) The effect of the HTF concentration on the I_{RRS} intensity of HSA at various concentrations of Nano-berberin. [HSA] = 4.5×10^{-3} mM, the concentration of HTF was 0 (○); 1.4 ×10^{-3} mM (●); 2.8×10^{-3} mM (□); 4.7 ×10^{-3}mM (■); 5.7×10^{-3} mM (Δ) and that of Nano-berberin increased from 0 to 6.52×10^{-3} mM. T=298K; pH = 7.4; phosphate buffer (50mM).

The RRS intensity can be calculated according to the following formula [68],

$$I_{RRS} = 32\pi^3 V^2 n^2 N / 3\lambda_0^4 \left[(\delta_n)^2 + (\delta_k)^2 \right] \quad (5)$$

where n is the refractive index of the medium, N is the molarity of the solution, λ_0 is the wavelength of the incident and scattered light, V^2 is the square of molecular volume, δ_n and δ_k are the fluctuations in the real and imaginary components of the refractive index of the particle, respectively. When other factors are constant, I_{RRS} is related to the size of the formed particle and directly proportional to the square of molecular volume (V^2). Apparently, with the increase of molecular volume, I_{RRS} is enhanced.

Figure (6B) displays the curves of ΔI_{RRS} versus different concentrations of Nano-berberin in the presence of holo-transferrin as $\Delta IRRS = I_{RRS} - I0_{RRS}$ (where IRRS and I0RRS are the RRS intensities of the systems with and without ligands). It can be seen that the enhancement of the RRS intensity differed for the various concentrations of holo-transferrin. When holo-transferrin was added to HSA-Nano-berberin, the RRS intensity became increased. It was determined that an interaction had occurred between HSA-Nano-berberin with holo-transferrin and that it resulted in an increase of the RRS signal. The enhanced RRS intensity was proportional to the molecular weight of the proteins. The RRS intensity of the HSA-Nano-berberin in the presence of holo-transferrin increased when raising the holo-transferrin concentration. When the Nano-berberin concentration was too low, the RRS intensity of the (HSA-Nano-berberin) holo-transferrin system hardly changed. However, with increasing Nano-berberin concentrations, the RRS intensity of the system gradually increased, and we could even observe that precipitation occurred in the solutions that contained high concentrations of Nano-berberin. The relationship between the RRS intensity and

the Nano-berberin concentration was nonlinear. In the graphs, the points where the curves crossed each other corresponded to the critical induced-aggregation concentration of Nano-berberin-induced protein aggregation ($\mathbf{C}_{\mathbf{CIAC}}$ values), as illustrated by (Figure 6B). Under identical experimental conditions, a smaller $\mathbf{C}_{\mathbf{CIAC}}$ value signified a smaller concentration of Nano-berberin-induced protein aggregation [69].

The addition of holo-transferrin to HSA-Nano-berberin also induced hydrophobic groups. The hydrophobic groups of the two-component complexes could interact with each other and aggregate together, which was the main reason for the enhanced RRS intensity of HSA. In addition, as shown in Figure (6B), when the Nano-berberin concentration reached about 2 $\times 10^{-3}$ mM, the Nano-berberin aggregated on the HSA, and this concentration value corresponded to the critical induced aggregation concentration (C_{CIAC}) of Nano-berberin [70,71].

CD spectroscopy

Since the late 1980s, there has been an explosive growth in structural biology with the number of high-resolution structures of proteins added to the protein data bank (PDB) currently expanding with more than 2000 per year. However, there is a growing realization of the need to perform structural studies under the conditions in which proteins actually operate (generally in solution), as well as under other conditions and to provide measures of the rates of structural changes of proteins, which are often essential to their biological function.

Circular dichroism (CD) has become increasingly recognized as a valuable structural technique for addressing these issues. CD spectra are immensely useful for studying three-dimensional structures of biopolymers such as proteins and nucleic acids. Each of the three basic secondary structures of a polypeptide chain (α-helix, β-sheet, and coil) shows a characteristic CD

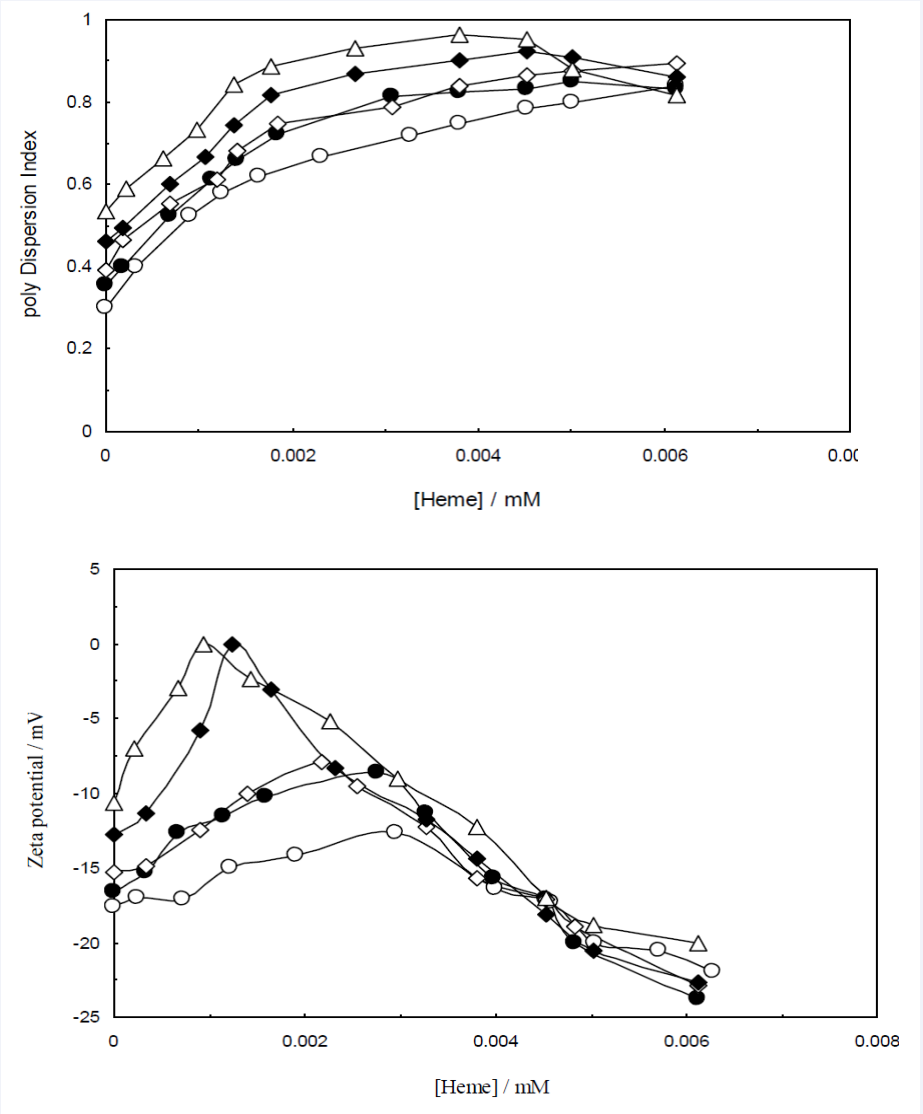

Figure 7 Far-UV CD spectra of HSA in the absence and presence of Nano-berberin and HTF at pH 7.4 and T = 298 K, [HSA] = 4.5× 10^{-3}mM. The Nano-berberin concentrations for the HSA-Nano-berberin system (from a to g), went from 0 to 6.52×10^{-3}mM and the HTF concentration increased from 0 to 5.7×10^{-3} mM for the far-UV CD measurements.

spectrum. For proteins, the aim is to analyze the CD spectra to obtain information of secondary structural features such as the percentage of α-helix or β-sheet or random coil regions. The CD signal is strong for α- helices and weak for β-sheets. It is very reliable for monitoring changes in the conformation of proteins under various conditions and for different drug binding types. In the unfolded state, CD is nearly zero in the region 210-220 nm, which corresponds to the absorption band of peptide bonds. Hence, protein folding/unfolding can be conveniently monitored by CD spectroscopy [72].

To obtain full comprehension of how the structure of HSA was affected by Nano-berberin in the absence and presence of holo-transferrin, CD measurements were performed on HSA, HSA-Nano-berberin, and (HSA- holo-transferrin) Nano-berberin complexes. Figure (7) shows the CD spectra of HSA and HSA-Nano-berberin with and without holo-transferrin. The CD spectra of HSA display two distinct negative minima in the ultraviolet region: one at 208 nm and the other at 222 nm, which are characteristic of an α-helical structure in a protein. A reasonable explanation is that the negative peaks at 208 and 222 nm both received contributions from n—› π* transfer for the peptide bond of the α-helix [73]. As can be seen from (Figure (7), the addition of Nano-berberin to HSA led to a decrease in the ellipticity without a significant shift of the peaks. It is true that in the HSA-Nano-berberin and (HSA- holo-transferrin) Nano-berberin complexes, the secondary structure of the protein changed. In the presence of holo-transferrin, the content of α-helix was reduced more than in the absence of holo-transferrin. However, the CD spectra of HSA in the presence and absence of Nano-berberin and holo-transferrin were similar in shape, indicating that the structure of HSA remained predominated by α-helices after the binding of Nano-berberin and holo-transferrin [74]. This suggested considerable changes in the secondary structure of HSA.

The α-helical content was calculated from Eq.(2) and the results revealed a decrease of α-helical structure from 53.97% to 42.28 % and 39.47% in the presence of Nano-berberin and holo-transferrin, respectively. In the presence of Nano-berberin, the α-helical content of HSA decreased, which indicated that hydrophobic interactions were predominant in the environment. In the presence of holo-transferrin, the α-helical content was reduced even further than in the absence of holo-transferrin. This means that holo-transferrin induced hydrophobic forces in the interaction between HSA and Nano-berberin. According to other reported studies [75], such a decrease in α-helical structure suggests a partial protein unfolding. Consequently, the increase in α-helical structure after Nano-berberin interaction in the binary system and holo-transferrin interaction in the ternary system should be a sign of decreased stability.

Zeta potential

Colloidal particles accumulate charges at their surfaces which can be expressed as a surface potential. This surface potential is an important factor for determining the magnitude of charged-based colloidal interactions of a particle, most likely electrostatic repulsion of other like charged particles. The surface charge on a particle perturbs the ionic distribution in the medium surrounding it. First, a layer of tightly bound counter-ions (i.e., of opposite charge) accumulates at the particle surface, the so-called Stern layer. Beyond this, a region of decaying excess concentration, the diffuse layer, extends a considerable distance into the surrounding aqueous media [76].

The measurement of the colloidal charge typically involves applying an electrical voltage to the particle and measuring the speed of movement induced. In practice, one or more layers of hydrated ions move with the particle and the potential determined is thus not that at the surface but rather at a short, undefined distance into the diffuse layer. It is called the zeta potential. The surface charge in protein particles is due to the partial ionization of various amino acid residues. The effective charge on a protein particle is affected by pH, ionic strength and the accumulation of ligands or surfactants at the interface [77].

The zeta -potential is calculated from the streaming potential using the Smoluchowski relationship [78]

$$Z = \Delta E/\Delta P = \eta\lambda/\varepsilon\varepsilon_0 \qquad (6)$$

where Z, η, λ, and $\varepsilon\varepsilon_0$ are respectively the zeta potential, the solution's viscosity, the solution's conductivity and the dielectric permittivity of water. ΔE/ΔP is the streaming potential, namely the slope of the curve of the difference in potential versus the difference in pressure.

The surface chemistry of biomaterials can have a significant impact on their performance in biological applications. Protein molecules adopt their native conformation in solution and within the cell only under specific environmental conditions. In order to confirm the existence of drug binding, zeta potential measurements were made at physiological pH. In this regard, the binding of the two ligands to HSA at pH 7.4 was expected to produce a change in the net charge on the protein–drug complexes provided that both the protein and the two ligands differed in their net electric charge at this pH (the isoelectric point of HSA is 4.9 [79]).

The influence of the varying concentrations of Nano-berberin holo-transferrin on the content of free amino groups on the capsule surface of HSA was analyzed. This is illustrated in (Figure 8), which shows a plot of the zeta potential of the protein–drug complexes as a function of the drug concentration. As the drug concentration increased, the initially negative charge of the protein was reduced, which suggests the formation of protein–drug complexes. This trend is also indicative of the existence of electrostatic interactions between the protein and the drug molecules [80-81]. At a determined and very high Nano-berberin concentration, there was a reversal in the sign of the zeta potential: it became positive until a zero region was reached. This point occurred approximately at a concentration of 2×10^{-3} mM of Nano-berberin, from which we can deduce that the formation of drug clusters or aggregates onto the protein had taken place.

From Figure 8, it can be seen that interactions occured between HSA and Nano-berberin or HOLO- holo-transferrin in the binary (□) and ternary (□,□,□,Δ) systems. This was also proven by the zeta potential of these systems at different concentrations

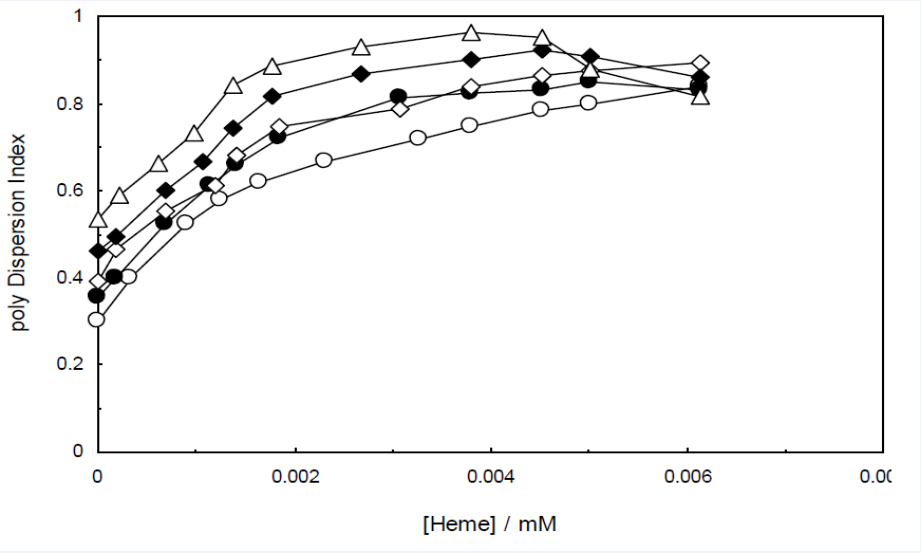

Figure 8 The dependence of the zeta-potential of HSA-Nano-berberin on the HTF concentration. (A), HSA-Nano-berberin(○); 1.4 ×10^{-3}mM (●); 2.8×10^{-3}mM (□); 4.7 × 10^{-3}mM (■); 5.7×10^{-3}mM (Δ), [HSA] = 4.5×10^{-3}mM and Nano-berberin increased from 0 to 6.52×10^{-3}mM. T=298K; PH = 7.4; phosphate buffer (50 mM).

of Nano-berberin and holo-transferrin. The zeta-potential values of HSA upon interaction with Nano-berberin and holo-transferrin in the ternary systems increased with raised concentrations of holo-transferrin and then decreased continuously. The inflection points of the zeta potential curves were similar to the $\mathbf{C_{CIAC}}$ values in Figure (6B). This means that when the Nano-berberin concentration was higher than $\mathbf{C_{CIAC,}}$ the hydrophobic interaction was predominant with a decrease in zeta potential. Therefore, the $\mathbf{C_{CIAC}}$ values illustrated the different behavior of Nano-berberin upon interaction with HSA, as confirmed by the zeta potential values.

Polydispersity index (PDI)

The ratio Mw/Mn is called the polydispersity or heterogeneity index [82]. The literature has shown that the amounts of protein and drug play a significant role when it comes to determining particle size, polydispersity and sample quality [83,84]. Polydispersity indicates the degree of nonuniformity of the particle size: it varies between 0 and 1. A low polydispersity (close to 0) indicates a greater uniformity in size distribution whereas a higher value (close to 1) indicates more nonuniformity. In addition to polydispersity, the quality of a sample is also related to its turbidity.

We tried to determine how the protein and the drugs were affected by these parameters. The dimensions, drug content, and polydispersity of various samples are shown in (Figure 9). For the samples with an increasing holo-transferrin concentration, the polydispersity index was close to 1 whereas HSA-Nano-berberin had a low polydispersity index near 0. This indicated that the degree of non uniformity of the particle size was increased when increasing the holo-transferrin concentration [85].

Molecular modeling

Although laboratory experiments may more closely represent physiological conditions, it is difficult to determine the location of the binding sites. An investigation of the 3D structure of crystalline albumin has shown that HSA contains three homologous domains (I–III): I (residues 1–195), II (196–383), and III (384–585); each domain has two subdomains (A and B). (Figure 10). The Autodock program was employed to examine the binding mode of Nano-berberin at the active site of HSA in the absence and presence of holo-transferrin.

In the docking process, only polar hydrogens were added to the protein and all water molecules were removed from the protein file in the AutoDock Tools software. The Lamarckian genetic algorithm (LGA) was utilized to calculate the conformational possibilities between the ligands and HSA. The docking parameter files for all docking procedures were generated by adopting the Lamarckian genetic algorithm method while the number of GA runs was set to 200 for each set. The population size was set to 150. The grid map was calculated using Autogrid and finally the best docking energy results were assumed as possible candidates for ligand protein interaction.

The best docking results of the interaction between Nano-berberin and HSA in the absence and presence of holo-transferrin, based on the lowest level of energy, are shown in (Table 6), which also lists the results of the drugs' interaction with HSA. The data was ranked by energy, and as shown in the table, holo-transferrin showed less affinity to the protein than Nano-berberin. When Nano-berberin and holo-transferrin docked solely onto the protein, they occupied the same pocket surrounded by hydrophobic residues in sub-domain IB (Leu115, Val116, Tyr161, Ala158) where it is possible to create hydrophobic interactions. However, the interactions between Nano-berberin and holo-transferrin to HSA were not exclusively hydrophobic in nature – there were also several ionic ones (Arg114, Arg186, Glu188) in the proximity of the bound ligand (within 5Å).

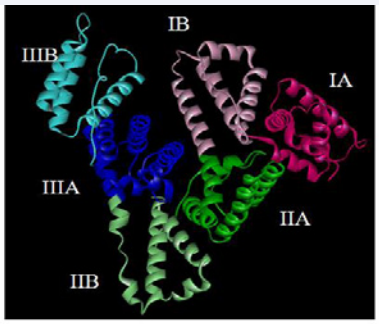

Figure 9 The dependence of the polydispersion of HSA-Nano-berberin on the HTF concentration. (A), HSA-Nano-berberin(○);1.4 $\times10^{-3}$ mM (●); 2.8$\times10^{-3}$ mM (□); 4.7$\times10^{-3}$ mM (■); 5.7$\times10^{-3}$ mM (Δ), [HSA] = 4.5$\times10^{-3}$ and Nano-berberin increased from 0 to 6.52$\times10^{-3}$ mM. T=298K; pH = 7.4; phosphate buffer (50 mM).

Figure 10 The native structure of HSA and the locations of its subdomains.

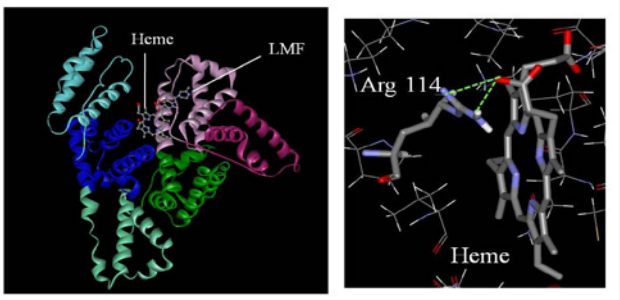

Figure 11 Docking interaction of (A), (HSA-Nano-berberin) HTF; (B), (HSA- HTF) Nano-berberin as ternary systems. The drugs are shown in ball-and-stick mode and the surface of the protein is colored according to the different subdomains.

In the next step, after the generation of binary systems for HSA-holo-transferrin and HSA-Nano-berberin, the ternary docking was performed following the energy minimization of the binary systems using a molecular mechanics method in the Hyperchem software, (Figure 11A,B). As shown in (Table 6), the inhibitory constant was decreased after addition of holo-transferrin to the HSA-Nano-berberin complex and it could therefore be concluded that the the initial binding of holo-transferrin enhanced the affinity of Nano-berberin to the protein. Moreover, we could see a further increase in affinity of Nano-berberin in the ternary system.

Several amino acids were involved in the hydrogen binding of holo-transferrin and Nano-berberin to the HSA. Examples include LEU283, Lys286, for holo-transferrin and Arg114, for Nano-berberin, which are the most important residues in this regard. In the ternary system, (HSA- holo-transferrin) Nano-berberin, holo-transferrin was able to form a hydrogen bond with Arg 114 and in (HSA-Nano-berberin) holo-transferrin, Nano-berberin could form hydrogen bonds with Arg 222 and Glu 153.

HSA contains a single Trp residue at position 214 in sub-domain IIA. The mentioned Trp was considered as the target to study the effect of the addition of drugs to HSA. As the efficient energy transfer from Trp214 to ligands was 2 - 8 nm, the distance of Trp 214 from the docked ligands was also measured. This was applicable with the high efficient fluorescence quenching of HSA emission in the presence of the second drug. As seen in (Table 7), the distance between Nano-berberin and holo-transferrin with Trp214 was about 2.2 and 2.3 nm, respectively, while in the ternary system of (HSA- holo-transferrin) Nano-berberin and (HSA-Nano-berberin) holo-transferrin, the corresponding values were 2.3 and 2.4 nm based on (Figure 12).

CONCLUSIONS

This paper presents spectroscopic studies on the interaction of Nano-berberin and holo-transferrin with HSA by multi-spectroscopic techniques, molecular modeling and zeta potential measurements. It was shown that the fluorescence of HSA was quenched upon interaction with Nano-berberin and holo-transferrin as a consequence of complex formation. The quenching belonged to the type static fluorescence quenching, with non-radiation energy transfer occurring within a single molecule.

The results revealed the presence of one type of binding site in the surroundings of the Trp and Tyr residues at the interface of HSA. The results of synchronous fluorescence spectroscopy and three-dimensional fluorescence spectra indicated that the environmental structure of the Trp residue was altered and that the physiological functions of HSA were affected by Nano-berberin and holo-transferrin. The aggregation of drug/protein complexes was determined through RRS and zeta-potential results. REES pointed at an obvious impact on the mobility of Trp. The binding of Nano-berberin and holo-transferrin to HSA changed the secondary structure of HSA, and it was shown that holo-transferrin-induced conformational changes could promote the interaction between HSA and Nano-berberin.

The binding properties of Nano-berberin and holo-transferrin to HSA were also mapped by molecular modeling. Docking calculations demonstrated that Nano-berberin and holo-transferrin were located in subdomain IB. The model showed that the attachment of holo-transferrin increased the affinity of Nano-berberin to HSA. A modulation of the Nano-berberin binding to HSA by drugs and metabolites was relevant in pharmacological therapy management. Indeed, the increase of the Nano-berberin plasma level under pathological conditions, such as severe hemolytic anemia, crash syndrome, and post-ischemic reperfusion, could induce the release of HSA-bound endogenous

Table 5: Fraction of secondary structure of HSA, and HSA-Nano-berberin in the presence and absence of different HOLO-TRANSFERRIN concentrations at pH=7.4.

System	f_α	f_β	f_T	f_u
HSA	53.97	18.31	13.48	14.25
HSA-Nano-berberin	42.28	11.04	8.25	38.43
(HSA-HTF, 1.4×10^{-3}mM)Nano-berberin	41.71	10.29	8.03	39.97
(HSA-HTF, 2.8×10^{-3}mM)Nano-berberin	39.47	9.14	6.93	44.46
(HSA-HTF, 4.7×10^{-3}mM)Nano-berberin	36.64	7.23	6.15	49.98
(HSA-HTF, 5.7×10^{-3}mM)Nano-berberin	31.55	5.32	5.74	57.39

Table 6: Best ranked results of the parameters for the interaction of HSA with Nano-berberin and AML in the binary and ternary systems at pH=7.4 by the Autodock procedure.

Sytem	Ki	Binding Energy (Kcal/mol)	Intermolecular Energy (Kcal/mol)	Electrostatic Energy (Kcal/mol)	Hydrogen bonds with
HSA-Nano-berberin	61.51 μM	-5.74	-8.25	-2.56	Arg114
(HSA-HTF) Nano-berberin	58.25 μM	-5.78	-8.13	-2.28	Arg114
HSA-HTF	92.19 μM	-5.51	-6.32	-1.29	Leu283 Lys 286
(HSA-Nano-berberin)HTF	88/86 μM	-5.53	-6.29	-2.85	Arg 222 Glu153

Table 7: The distance of Trp 214 with Nano-berberin and HTF and also between Nano-berberin and HTF in binary and ternary systems.

Distance in systems	Nano-berberin and Trp214	HTF and Trp214	Nano-berberin and HTF
HSA-Nano-berberin	2.2 nm	____	____
(HSA- HTF)Nano-berberin	0.7 nm	2.3 nm	0.5 nm
HSA- HTF	____	2.4 nm	___
(HSA-Nano-berberin) HTF	2.3 nm	0.5 nm	0.7 nm

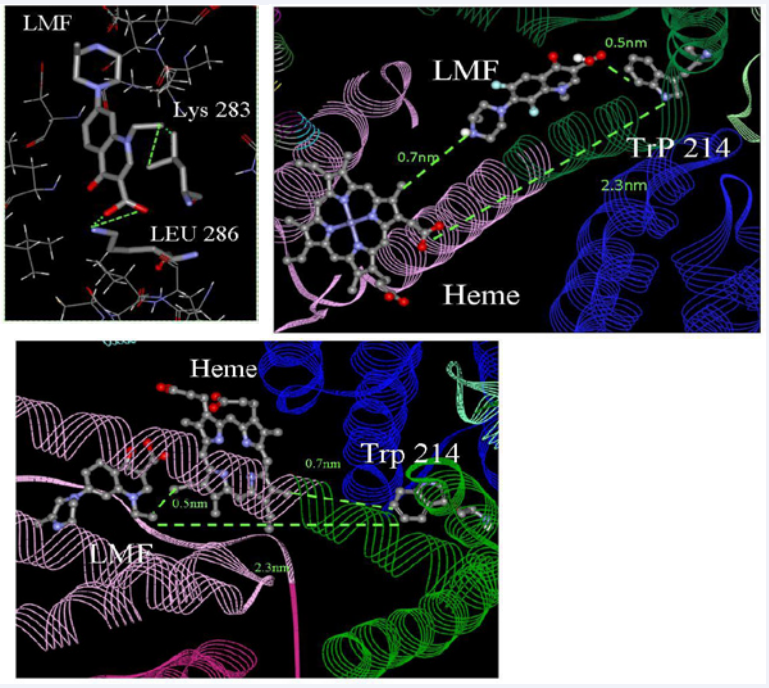

Figure 12 (A) The computational model of the docking; (A). The hydrogen bonds between the residues of HSA with Nano-berberin, (B): The hydrogen bonds between the residues of HSA with HTF are represented by green dashed lines, (C) The distances between the Trp 214 of HSA in (HSA-Nano-berberin) HTF; (D), and (HSA- HTF) Nano-berberin systems.

and exogenous ligands (e.g., metabolites and drugs) increasing their bio-availability with the concomitant intoxication of the patient.

Lastly, data available for HSA-Nano-berberin described a curious situation where the binding of Nano-berberin to a non-classical Nano-berberin-protein (HSA) conferred (although transiently) ligand binding and (pseudo-) enzymatic properties. One should note that the effects arising from Nano-berberin binding to HSA might have a role in the regulation of biological functions. Since these actions are dependent on the transient interaction of a ligand (Nano-berberin) with a carrier (HSA), they have been called "chronosteric" effects.

ACKNOWLEDGEMENTS

The financial support of the Research Council of the Mashhad Branch, Islamic Azad University is gratefully acknowledged. The authors thank Dr. Ljungberg for the English editing.

REFERENCES

1. Tuszynski JA, Kurzynski M (2003) Structure of Biomolecules. CRC Press in PURe and Applied physics.
2. Vuignier K, Schappler G, Veuthery JL, Carrupt PA, Martel S (2010) Improvement of a capillary elecrtrophoresis/ frontal analysis (CE/FA) method for determining binding constant: Discussion on relevant parameters. J Pharm Biomed Anal.2010 ; 53(5) :1288-1297.
3. Peters TJ (1996) All about Albumin. San dirgo, Academic press. 1996; 41: 382-382.
4. Nicholson JP, Wolmarans MR, Park GR, British J (2000) The role of albumin in critical illness. J Anaesth 2000; 85 :599-610.
5. Ponka P (1999) Cell biology of Nano-berberin. J Med Sci 318: 241-256.
6. Dawson JH, (1988) Probing Structure-function relation in Nano-berberin containing oxygenases and peroxidases. J Science 240 : 433-439.
7. Bandyopadhyay U, Biswas K, Banerjee RK (1992) Extrathyroidal action of antithyroid thionamides. Toxicol Lett. 2002; 128 :117-128.
8. Sears DA (1970) Disposal of plasma Nano-berberin in normal man and patients with intravascular hemolysis. J clin invest 49 : 5-14
9. Sassa S (1976) Sequential induction of Nano-berberin pathway enzymes during erythroid differentiation of mouse Friend leukemia virusinfected cells. J Exp Med 143: 305-315.
10. Gidari AS, Levere RD (1977) Enzymatic formation and cellular regulation of Nano-berberin synthesis. J Semin Hematol 14: 145-168.
11. Benz EJ, Murnane MJ, Tonkonow BL, Berman BW. Mazur EM, Cavallesco C, Jenko T, Snyder EL (1980) Embryonic–fetal erythroid characteristics of a human leukemiccell line. Proc Natl Acad Sci USA 1980 ;77 :3509-3513
12. Ascenzi P, Bocedi A, Visca P, Altruda F, Tolosano E, Beringhelli T, Fasano M (2005) Hemoglobin and Nano-berberin scavenging. IUBMB Life 57 :749-759.
13. Fasano M, Curry S, Terreno E, Galliano M, Fanali G, Narciso P, Notari S, Ascenzi P (2005) The extraordinary ligand binding properties of human serum albumin. IUBMB Life 2005 ; 57(12) :787-796.
14. Ascenzi P, Bocedi A, Notari S, Fanali G, Fesce R, Fasano M (2006) Allosteric modulation of drug binding to human serum albumin. Mini Rev Med Chem.2006; 6 : 483-489.
15. Yang F, Bian C, Zhu L, Zhao G, Huang Z, Huang M (2007) Effect of human serum albumin on Drug metabolism: structural evidence of esterase activity of human serum albumin. J Struct Biol.2007 ; 157(2) :348-355.
16. Ascenzi P, Fasano M (2009) Serum Nano-berberin-albumin: an allosteric protein. IUBMB Life.2009 ; 61(12) :1118-1122.
17. Abraham NG (1991) Molecular regulation: biological role of Nano-berberin in hematopoiesis. Blood Rev 5: 19-28.
18. Ascenzi P, Gullotta F, Gioia M, Coletta M, Fasano M (2011) O_2 – mediated oxidation of ferrous nitrosylated human serum Nano-berberin-albumin is limited by nitrogen monoxide dissociation. J Biochem Biophys Research commun.2011 ;406(1) :112-116.
19. Tsiftsoglou AS, Tsamadou AI, Papadopoulou C (2006) Nano-berberin as Key regulator of major mammalian cellular function: Molecular, Cellular, and pharmacological aspect. J clin Pharma Ther 111:327-345.
20. Trynda- Lemesz L (2004) Paclitaxel-HSA interaction. Binding sites on HSA molecule.J Bioorg Med Chem.2004 ; 12(12) :3269-3275.
21. Grinberg LN, O'Brien PJ, Hrkal Z, (1999) The Effect of Nano-berberin-Binding protein on the peroxidative and catalatic activities of hemin. J Free Radica Biol Med 26:214-219.
22. Van Langendonck AV, Casanas-Roux F, Dolmans MM, Donnez J (2002) Potential involvement of hemoglobin and Nano-berberin in the pathogenesis of peritoneal endometriosis. Fertil Steril 77: 561-570.
23. Mattu M, Vannini A, Coletta M, Fasano M, Ascenzi P (2001) Effect of bezafibrate and clofibrate on the Nano-berberin-iron geometry of ferrous nitrosylated Nano-berberin-human serum: an EPR study. J Inorg Biochem. 2001 ;84(3-4) :293-296.
24. Pamplona A, Ferreira A, Balla J, Jeney V, Balla G, Epiphanio S, Chora A, Rodrigues CD, Gregoire IP, Cunha-Rodrigues M, Portugal S, Soares MP, Mota MM (2007) Nano-berberin oxygenase-1 and carbon monoxide suppress the pathogenesis of experimental cerebral malaria. Nature Med 13: 703–710.
25. Solar I, Muller-Eberhard U, Shaklai N (1989) Serum proteins as mediators of hemin efflux from red Cell membranes: specificity of hemopoxin. Febs Lett 256:225-229.
26. Rubinstein E (2001) History of quinolones and their side effects. Chemotherapy.2001 ; 47: 3:3–8:44-48
27. Freeman CD, Nicolau DP, Belliveav PP (1993) Nightingle CD Lomefloxacin clinical pharmacokinetics. Clinical Pharmcokinet.1993 ; 25(1): 6-19.
28. Seedher N, Bhatia S (2006) Reversible binding of celecoxib and valdecoxib with human serum albumin using fluorescence spectroscopic technique. Pharmacol Res.2006 :54(2) :77–84.
29. Anbazhagan V, Renganathan R (2008) Study on the binding of 2,3-diazabicyclo[2.2.2.]oct-2-ene with bovin serum albumin by fluorescence spectroscopy. Journal of Luminescence.2008; 128(9): 1454-1458.
30. Ding F, Huang J, Lin J, Li Z, Liu F, Jiang Z, Sun Y (2009) A study of the binding of C.I. Mordant Red 3 with bovin serum albumin using fluorescence spectroscopy. Dyes and Pigments.2009 ; 82(1) : 65-70.
31. wang T, Xiang BR, Li Y, Chen CY, Zhou XH (2009) Studies on the binding of a cardiotic agent to human serum albumin by two-dimentional correlation fluorescence spectroscopy and molecular modeling. J Mol Struct 921:188-198.
32. Eftink M R(1991) In Methods of Biochemical Analysis. Suelter C H, John Wiley, New York.
33. Lakowicz JR (2006) In Principles of Fluorescence Spectroscopy.

Kluwer-Plenum, New York.

34. Ross JBA, Laws WR, Rousslang K W, Wyssbrod HR (1992) Topics in Fluorescence. Spectroscopy. Lakowicz JR, Plenum Press, New York.

35. Ladokhin AS (2000) Encyclopedia of Analytical Chemistry. Meyers, John Wiley, Chichester.

36. Rinco O, Brenton J, Douglas A, Maxwell A, Henderson A (2009) The effect of porphyrin structure on binding to human serum albumin by fluorescence spectroscopy. J Photochemistry and Photobiolology A Chemistry. 2009 ; 208(2) : 91-96.

37. Yuan J.L, Lv Z, LiuZG, Hu Z, Zou GL (2007) Study interaction between apigenin and human serum albumin by spectroscopy and molecular modeling. J Photochemistry and Photobiolology A Chemistry.2007 ; 191(2) :104-113.

38. Jiang M, Xie MX, Zheng D, Liu Y, Li XY, Chen X, (1973) Spectroscopic studies on the interaction of cinnamic acid and its hydroxyl derivatives with human serum albumin. J.molstruc.2004 ; 692(1-3) :71–80.

39. Lakowicz JR, Weber G (1973) Quenching of fluorescence by oxygen. Probe for structural fluctuations in macromolecules. Biochemistry.1973 ;12(21) :4161-4170.

40. Ware WR (1962) Oxygen quenching of fluorescence in solution: an experimental study of the diffusion process. J Phys.Chem. 1962 ; 66(3) :455–458.

41. Hu YJ, Liu Y, Wang JB, Xiao XH, Qu SS (2004) Study of the interaction between Monoammonium glycyrrhizinate and bovine serum albumin. J Pharm Biomed Anal. 2004 ; 36(4) :915–919.

42. Qi ZD, Zhou B, Xiao Q, Shi C, Liu Y, Dai J (2008) Interaction of rofecoxib with human serum albumin: determination of binding constants and the binding site by spectroscopic methods. J Photochem.2008; 193(2-3):81–88.

43. Kandagal PB, Kalanur SS, Manjunatha DH, Seetharamappa J (2008) Mechanism of interaction between human serum albumin and N-alkyl phenothiazines studied using spectroscopic methods. J Pharm Biomed Anal. 2008 ; 47(2) :260–267.

44. Lakowicz JR, Weber G (1973) Quenching of protein fluorescence by oxygen. Detection of structural fluctuations in proteins on the nanosecond time scale. Biochemistry.1973; 12(21): 4171–4179.

45. Lakowicz JR (2006) Principle of Fluorescence Spectroscopy, Springer Science+Business Media, New York.

46. Lloyd JBF, Evett IW (1977) Prediction of peak wavelengths and intensities in synchronously excited fluorescence emission spectra. Anal.Chem.1977 ; 49(12) :1710-1715.

47. Lloyd JBF (1980) Limitations of synchronous luminescence spectrometry in multicomponent analysis. Anal.Chem.1980 ; 52(1) :189-191.

48. Yuan T, Weljie AM, Vogel HJ (1998) Tryptophan fluorescence quenching by methionine and selenomethionine residues of calmodulin: orientation of peptide and protein binding. Biochemistry.1998; 37(9) :3187-3195.

49. Abert WC, Gregory WM, Allan GS (1993) The binding interaction of coomassie blue with protein. Anal Biochem.1993 ; 213(2) :407-413.

50. Hu YJ, Liu Y, Pi ZB, Qu SS (2005) Interaction of cromolyn sodium with human serum albumin: a fluorescence quenching study. Bioorg Med Chem.2005 ;13(24) :6609-6614.

51. Wang YQ, Zhang HM, Zhang GC, Zhou QH, Fei ZH, Liu ZT (2008) Fluorescence spectroscopic investigation of the interaction between benzidine and bovine hemoglobin. J of Molecular Structure.2008; 886(1-3) :77–84.

52. Hu X, Cui S, Liu JQ (2010) Fluorescence studies of interaction between flavonol P-coumaroylglucoside tiliroside and bovin serum albumin. Spectrochim Acta A Mol Biomol Spectrosc.2010; 77(2) :548-553.

53. Zhang G, Que Q, Pan J, Guo J (2008) Study of the interaction between icariin and human serum albumin by fluorescence spectroscopy. Journal of Molecular Structure.2008 ; 881(1-3) :132-138.

54. Ding F, Liu W, LI Y, Sum Y (2010) Determining the binding affinity and binding site of bensulfuron-.methyl to human serum albumin by quenching of the intrinsic tryptophan fluorescence. 2010 : 130(11) : 2013-2021.

55. Shi X, Li X, Gui M, Zhou H, Yang R, Zhang H, Jin Y (2010) Studies on interaction between flavonoids and bovine serum albumin by spectral methods. Lumin 130:637-644.

56. Y-qing W, Bio-Ping T, Hong-mei Z,Q-Hua Z, Gen-cheng Z (2009) Studies on the interaction between imidacloprid and human serum albumin:Spectroscopic approach. Journal of photochemistryand Photobiology B: Biology. 2009 ; 94(3) :183-190.

57. Overton MC, Blumer KJ, (2002) Use of fluorescence resonance energy transfer to analyze oligomerization of G-protein-coupled receptors expressed in yeast. Methods.2002 ; 27(4) :324-332.

58. Schuler B (2005) Single-Molecule Fluorescence Spectroscopy of Protein Folding. ChemPhys Chem. 2005 ;6(7) :1206-1220.

59. Zhang H, Wang Y.Q, Jiang ML (2009) A fluorimetric study of the interaction of C.I. Solvent Red 24 With Haemoglobin. Dyes and Pigments. 2008 ; 82(2) :156-163.

60. Tory M C, Rod Miller A (2002) Determination of membrane protein topology by red-edge excitation shift analysis: application to the membrane-bound colicin E1 channel peptide. Biochem et Biophys Acta(BBA).2002 ; 1546(2) :435-448.

61. Klajnert B, Stanislawska L, Bryszewska M, Palecz B (2003) Interactions between PAMAM dendrimers and bovine serum albumin. Biochem Biophys Acta.2003 ; 1648(1-2) :115–126.

62. Cosa T, Seixas Melo J (2009) A resonance Rayleigh scattering study of unlabeled and pyrene-labeled poly(acrylic acid) polymers. Journal of Molecular Structure.2009 ; 920:142-148.

63. Li J, Li M, Li X, Tang J, Zhang H, Zhang Y (2008) Study on the resonance light-scattering spectrum of lysozyme-DNA /CdTe nonaparticles system. J Colloids Sur B Biointerface.2008 ; 67(1) :79-84.

64. Cui F, Wang L, Cui Y (2007) Determination of bismuth in pharmaceutical products using methyltriphenylphosphonium bromide as a molecular prob by resonance light scattering technique. J Pharm Biomed Anal.2006 ; 43(3) :1033-1038.

65. Li J, Li M, Tang J, Li Hanqi, Zhang Y (2008) Resonance light-scattering spectrometric study of interaction between enzyme and MPA-modified CdTe nanoparticles. Spectrochim Acta part A Mol Biomol Spectrosc 70:514-518.

66. Chen Z, Li Z, Song T, Chen J, Guo Z (2009) A novel curcumin assay with the metal ion cu(II) as a simple prob by resonance light scattering technique. Spectrochim Acta part A: Molecular and Biomoleculart Spectroscopy.2009 ; 72(3) :518-522.

67. Chen Z, Peng Y, Chen J, Zhu L (2008) Determination of antibacterial quaternary ammonium compound in lozenges and human serum by resonance light scattering technique. J pharm Biomed Anal.2008 ; 48(3) :946-950.

68. Li L, Shun Z, Pan Q, Wu Song G (2009) Determination of nucleic acid based on increased resonance light-scattering of fluorinated surfactants. Journal of Fluorine Chemistry.2009 ; 130(6): 567-572.

69. Qin M,Liu S, Liu Z, Hu X (2009) Resonance Rayleigh scattering

spectra,non-linear scattering spectra of tetracaine hydrochloride-erythrosin system and its analytical application. Spectrochima Acta part A: Molecular and Biomolecular Spectroscopy.2009 ; 71(5) :2063-2068.

70. Long X, Zhang C, Cheng J, Bi S (2008) A novel method for study of the aggregation of protein induced by metal ion aluminum (III) using resonance Rayleigh scattering teqnique. Spectrochim Acta A Mol Biomol Specrosc. 2008 ; 69(1) :71-77.

71. Chamani J, Vahedian-Movahed H, Saberi M R (2011) Lomefloxacin promotes the interaction between human serum albumin and transferrin: A mechanistic insight into the emergence of antibiotic's side effects. J Pharm Biomed Anal.2011 ; 55(1) :114-124.

72. Kelly S M, Jess T J, Price N C (2005) How to study proteins by circular dichroism. Biochima et Biophysica Acta (BBA) Proteins and Proteomics.2005 ; 1751(2): 119 – 139.

73. Yuan J, Liu H, Kang X, Zou GL (2008) Characteristics of the isomericflavonoids apigenin and genistein binding to hemoglobin by spectroscopic methods. Journal of Molecular Structure.2008; 891(1-3) : 333-339.

74. Song S M, Hou XL, Wu Y B, Shuang SM, Yang C, Inoue Y, Dong C (2009) Study on the interaction between methyl blue and human serum albumin by fluorescence spectroscopy. Journal of Luminescence. 2009 ; 129 :169-175.

75. Wang Y.Q, Zhang H M, Zhou Q H, Xu H L (2009) A study of the binding of colloidal Fe3O4 with bovine hemoglobin using optical spectroscopy. Colloids and Surfaces A: Physicochemical and Engineering Aspects. 2009 ; 337(1-3):102–108.

76. Malhotra A , Coupland J N, (2004) The effect of surfactant on the solubility, zeta potential, and viscosity of soy protein isolated. Food Hydrocolloids. 2004 ; 18(1) :101-108.

77. Koch S,Woias P, Meixner K, Drost S, Wolf H, Biosen J (1999) Protein detection with a novel ISFET-based zeta potential analyzer. Biosens Bioelectron.1999 ; 14(4) : 413-421.

78. Bernsmans F , Frisch B, Ringwald C, Ball V (2010) Protein adsorption on dopamine–melanin films: Role of electrostatic interactions inferred from f-potential measurements versus chemisorption J Colloids Interface sci.2010 ; 344(1) :54-60.

79. Weber C, Coester C, Kreuter J, Langer K (2000) Desolvation process and surface characterisation of protein nanoparticle. Int J Pharm.2000; 194(1) :91-102.

80. Wiacek AE, Chiowski E (2005) Zeta potential and droplet size of *n*-tetradecane/ethanol (protein) Emulsions. Colloids and surfaces B: Biointerfaces.2002 ; 25(1) :55-67.

81. Atkins P W (2001) Physical Chemistry, Oxford university press.

82. Liu CH, Yu SU (2010) Cationic nanoemulsions as non-viral vectors for plasmid DNA delivery. Colloids Surf B Biointerfaces. 2010 ; 79(2) :509-515.

83. Olivera A C, Ferraz M P, Monterio FJ, Simo S (2009) Cationic liposome–DNA complexes as gene delivery vectors:Development and behaviour towards bone-like cells. Acta Biomaterial 5 :2142-2151.

84. Li D, Ji B, Sun H (2009) Probing the binding of 8-Acetyl-7-hydroxycoumarin to human serum albumin by spectroscopic methods and molecular modeling. Spectrochim Acta A Mol Biomol Spectrosc. 2009 ; 73(1) :35-40.

85. Chamani J, Assodeh A, Homayoni-Tabrizi M, Amiri Tehranizadeh Z, Baratian A, Saberi MR, Gharanfoli M (2010) Spectroscopic and nano-molecular modeling investigation on the binary and ternary bindings of colchicine and lomefloxacin to Human serum albumin with the viewpoint of multi-drug therapy. Journal of Luminescence.2010; 130(12) :2476-2486.

Cite this article

Sharifi-Rad A, Mehrzad J, Darroudi M, Saberi MR, Chamani J (2021) Reduction of Nano-berberin affinity to human serum albumin in the presence of holo-transferrin: Spectroscopic, zeta potential and molecular modeling investigations. J Clin Pharm 5(1): 1017.